

Higher-Order Spectral Clustering of Directed Graphs

Steinar Laenen *

Oxford Research Group
FiveAI
steinar.laenen@five.ai

He Sun

School of Informatics
University of Edinburgh
h.sun@ed.ac.uk

Abstract

Clustering is an important topic in algorithms, and has a number of applications in machine learning, computer vision, statistics, and several other research disciplines. Traditional objectives of graph clustering are to find clusters with low conductance. Not only are these objectives just applicable for undirected graphs, they are also incapable to take the relationships between clusters into account, which could be crucial for many applications. To overcome these downsides, we study directed graphs (digraphs) whose clusters exhibit further “structural” information amongst each other. Based on the Hermitian matrix representation of digraphs, we present a nearly-linear time algorithm for digraph clustering, and further show that our proposed algorithm can be implemented in sublinear time under reasonable assumptions. The significance of our theoretical work is demonstrated by extensive experimental results on the UN Comtrade Dataset: the output clustering of our algorithm exhibits not only how the clusters (sets of countries) relate to each other with respect to their import and export records, but also how these clusters evolve over time, in accordance with known facts in international trade.

1 Introduction

Clustering is one of the most fundamental problems in algorithms and has applications in many research fields including machine learning, network analysis, and statistics. Data can often be represented by a graph (e.g., users in a social network, servers in a communication network), and this makes graph clustering a natural choice to analyse these datasets. Over the past three decades, most studies on undirected graph clustering have focused on the task of partitioning with respect to the edge densities, i.e., vertices form a cluster if they are better connected to each other than to the rest of the graph. The well-known normalised cut value [25] and graph conductance [20] capture these classical definitions of clusters, and have become the objective functions of most undirected graph clustering algorithms.

While the design of these algorithms has received a lot of research attention from both theoretical and applied research areas, these algorithms are usually unable to uncover higher-order structural information among clusters in directed graphs (digraphs). For example, let us look at the international oil trade network [29], which employs digraphs to represent how mineral fuels and oils are imported and exported between countries. Although this highly connected digraph presents little cluster structure with respect to a typical objective function of undirected graph clustering, from an economic point of view this digraph clearly exhibits a structure of clusters: there is a cluster of countries mainly exporting oil, a cluster mainly importing oil, and several clusters in the middle of this trade chain. All these clusters are characterised by the imbalance of the edge directions between clusters, and further present a clear ordering reflecting the overall trade pattern. This type of structure is not only found in trade data, but also in many other types of data such as migration data and infectious disease

*steinar9@gmail.com

spreading data. We view these types of patterns as a *higher-order* structure among the clusters and, in our point of view, this structural information could be as important as the individual clusters themselves.

Our contribution. In this work we study clustering algorithms for digraphs whose cluster structure is defined with respect to the imbalance of edge densities as well as the edge directions between the clusters. Formally, for any set of vertices S_0, \dots, S_{k-1} that forms a partition of the vertex set $V(G)$ of a digraph G , we define the *flow ratio* of $\{S_j\}_{j=0}^{k-1}$ by

$$\sum_{j=1}^{k-1} \frac{w(S_j, S_{j-1})}{\text{vol}(S_j) + \text{vol}(S_{j-1})},$$

where $w(S, T) \triangleq \sum_{\substack{(u,v) \in E \\ u \in S, v \in T}} w(u, v)$ is the cut value from $S \subset V$ to $T \subset V$ and $\text{vol}(S)$ is the sum of degrees of the vertices in S . We say that $\{S_j\}_{j=0}^{k-1}$ forms an optimal partition if this $\{S_j\}_{j=0}^{k-1}$ maximises the flow ratio over all possible partitions. By introducing a complex-valued representation of the graph Laplacian matrix \mathcal{L}_G , we show that this optimal partition $\{S_j\}_{j=0}^{k-1}$ is well embedded into the bottom eigenspace of \mathcal{L}_G . To further exploit this novel and intriguing connection, we show that an approximate partition with bounded approximation guarantee can be computed in time nearly-linear in the number of edges of the input graph. In the settings for which the degrees of the vertices are known in advance, we also present a sub-linear time implementation of the algorithm. The significance of our work is further demonstrated by experimental results on several synthetic and real-world datasets. In particular, on the UN Comtrade dataset our clustering results are well supported by the literature from other research fields. At the technical level, our analysis could be viewed as a hybrid between the proof of the Cheeger inequality [6] and the analysis of spectral clustering for undirected graphs [23], as well as a sequence of recent work on fast constructions of graph sparsification (e.g., [26]). We believe our analysis for the new Hermitian Laplacian \mathcal{L}_G could inspire future research on studying the clusters' higher-order structure using spectral methods.

Related work. There is a rich literature on spectral algorithms for graph clustering. For undirected graph clustering, the works most related to ours are [23, 25, 30]. For digraph clustering, [24] proposes to perform spectral clustering on the symmetrised matrix $A = M^\top M + M M^\top$ of the input graph's adjacency matrix M ; [9] initiates the studies of spectral clustering on complex-valued Hermitian matrix representations of digraphs, however their theoretical analysis only holds for digraphs generated from the stochastic block model. Our work is also linked to analysing higher-order structures of clusters in undirected graphs [4, 5, 31], and community detection in digraphs [7, 21]. The main takeaway is that there is no previous work which analyses digraph spectral clustering algorithms to uncover the higher-order structure of clusters in a general digraph.

2 Preliminaries

Throughout the paper, we always assume that $G = (V, E, w)$ is a digraph with n vertices, m edges, and weight function $w : V \times V \rightarrow \mathbb{R}_{\geq 0}$. We write $u \rightsquigarrow v$ if there is an edge from u to v in the graph. For any vertex u , the in-degree and out-degree of u are defined as $d_u^{\text{in}} \triangleq \sum_{v: v \rightsquigarrow u} w(v, u)$ and $d_u^{\text{out}} \triangleq \sum_{v: u \rightsquigarrow v} w(u, v)$, respectively. We further define the total degree of u by $d_u \triangleq d_u^{\text{in}} + d_u^{\text{out}}$, and define $\text{vol}(S) \triangleq \sum_{u \in S} d_u$ for any $S \subseteq V$. For any set of vertices S and T , the symmetric difference between S and T is defined by $S \triangle T \triangleq (S \setminus T) \cup (T \setminus S)$.

Given any digraph G as input, we use $M \in \mathbb{R}^{n \times n}$ to denote the adjacency matrix of G , where $M_{u,v} = w(u, v)$ if there is an edge $u \rightsquigarrow v$, and $M_{u,v} = 0$ otherwise. We use $A \in \mathbb{C}^{n \times n}$ to represent the Hermitian adjacency matrix of G , where $A_{u,v} = \overline{A_{v,u}} = w(u, v) \cdot \omega_{\lceil 2\pi k \rceil}$ if $u \rightsquigarrow v$, and $A_{u,v} = 0$ otherwise. Here, $\omega_{\lceil 2\pi k \rceil}$ is the $\lceil 2\pi k \rceil$ -th root of unity, and \bar{x} is the conjugate of x . The normalised Laplacian matrix of G is defined by $\mathcal{L}_G \triangleq I - D^{-1/2} A D^{-1/2}$, where the degree matrix $D \in \mathbb{R}^{n \times n}$ is defined by $D_{u,u} = d_u$, and $D_{u,v} = 0$ for any $u \neq v$. We sometimes drop the subscript G if the underlying graph is clear from the context.

For any Hermitian matrix $A \in \mathbb{C}^{n \times n}$ and non-zero vector $x \in \mathbb{C}^n$, the Rayleigh quotient $\mathcal{R}(A, x)$ is defined as $\mathcal{R}(A, x) \triangleq x^* A x / x^* x$, where x^* is the complex conjugate transpose of $x \in \mathbb{C}^n$. For any

Hermitian matrix $B \in \mathbb{C}^{n \times n}$, let $\lambda_1(B) \leq \dots \leq \lambda_n(B)$ be the eigenvalues of B with corresponding eigenvectors f_1, \dots, f_n , where $f_j \in \mathbb{C}^n$ for any $1 \leq j \leq n$.

3 Encoding the flow-structure into \mathcal{L}_G 's bottom eigenspace

Now we study the structure of clusters with respect to their flow imbalance, and their relation to the bottom eigenspace of the normalised Hermitian Laplacian matrix. For any set of vertices S_0, \dots, S_{k-1} , we say that S_0, \dots, S_{k-1} form a k -way partition of $V(G)$, if it holds that $\bigcup_{0 \leq j \leq k-1} S_j = V(G)$ and $S_j \cap S_\ell = \emptyset$ for any $j \neq \ell$. As discussed in Section 1, the primary focus of the paper is to study digraphs in which there are significant connections from S_j to S_{j-1} for any $1 \leq j \leq k-1$. To formalise this, we introduce the notion of *flow ratio* of $\{S_j\}_{j=0}^{k-1}$, which is defined by

$$\Phi_G(S_0, \dots, S_{k-1}) \triangleq \sum_{j=1}^{k-1} \frac{w(S_j, S_{j-1})}{\text{vol}(S_j) + \text{vol}(S_{j-1})}. \quad (1)$$

We call this k -way partition $\{S_j\}$ an *optimal clustering* if the flow ratio given by $\{S_j\}$ achieves the maximum defined by

$$\theta_k(G) \triangleq \max_{\substack{S_0, \dots, S_{k-1} \\ \bigcup S_i = V, S_j \cap S_\ell = \emptyset}} \Phi_G(S_0, \dots, S_{k-1}). \quad (2)$$

Notice that, for any two consecutive clusters S_j and S_{j-1} , the value $w(S_j, S_{j-1}) \cdot (\text{vol}(S_j) + \text{vol}(S_{j-1}))^{-1}$ evaluates the ratio of the total edge weight in the cut (S_j, S_{j-1}) to the total weight of the edges with endpoints in S_j or S_{j-1} ; moreover, only $k-1$ out of $2 \cdot \binom{k}{2}$ different cuts among S_0, \dots, S_{k-1} contribute to $\Phi_G(S_0, \dots, S_{k-1})$ according to (1). We remark that, although the definition of $\Phi_G(S_0, \dots, S_{k-1})$ shares some similarity with the normalised cut value for undirected graph clustering [25], in our setting an optimal clustering is the one that *maximises* the flow ratio. This is in a sharp contrast to most objective functions for undirected graph clustering, whose aim is to find clusters of low conductance². In addition, it is not difficult to show that this problem is NP-hard since, when $k=2$, our problem is exactly the MAX DICUT problem studied in [15].

To study the relationship between the flow structure among S_0, \dots, S_{k-1} and the eigen-structure of the normalised Laplacian matrix of the graph, we define for every optimal cluster S_j ($0 \leq j \leq k-1$) an indicator vector $\chi_j \in \mathbb{C}^n$ by $\chi_j(u) \triangleq (w_{\lceil 2\pi \cdot k \rceil})^j$ if $u \in S_j$ and $\chi_j(u) = 0$ otherwise. We further define the normalised indicator vector of χ_j by

$$\widehat{\chi}_j \triangleq \frac{D^{1/2} \chi_j}{\|D^{1/2} \chi_j\|},$$

and set

$$y \triangleq \frac{1}{\sqrt{k}} \sum_{j=0}^{k-1} \widehat{\chi}_j. \quad (3)$$

We highlight that, due to the use of complex numbers, a single vector y is sufficient to encode the structure of k clusters: this is quite different from the case of undirected graphs, where k mutually perpendicular vectors are needed in order to study the eigen-structure of graph Laplacian and the cluster structure [20, 23, 30]. In addition, by the use of roots of unity in (3), different clusters are separated from each other by angles, indicating that the use of a single eigenvector could be sufficient to approximately recover k clusters. Our result on the relationship between $\lambda_1(\mathcal{L}_G)$ and $\theta_k(G)$ is summarised as follows:

Lemma 3.1. *Let $G = (V, E, w)$ be a weighted digraph with normalised Hermitian Laplacian $\mathcal{L}_G \in \mathbb{C}^{n \times n}$. Then, it holds that $\lambda_1(\mathcal{L}_G) \leq 1 - \frac{4}{k} \cdot \theta_k(G)$. Moreover, $\theta_k(G) = k/4$ if G is a bipartite digraph with all the edges having the same direction, and $\theta_k(G) < k/4$ otherwise.*

²It is important to notice that, among $2 \cdot \binom{k}{2}$ cuts formed by pairwise different clusters, only $(k-1)$ cut values contribute to our objective function. If one takes all of the $2 \cdot \binom{k}{2}$ cut values into account, the objective function would involve $2 \cdot \binom{k}{2}$ terms. However, even if most of the $2 \cdot \binom{k}{2}$ terms are much smaller than the ones along the flow, their sum could still be dominant, leaving little information on the structure of clusters. Therefore, we should only take $(k-1)$ cut values into account when the clusters present a flow structure.

Notice that the bipartite graph G with $\theta_k(G) = k/4$ is a trivial case for our problem; hence, without loss of generality we assume $\theta_k(G) < k/4$ in the following analysis. To study how the distribution of eigenvalues influences the cluster structure, similar to the case of undirected graphs we introduce the parameter γ defined by

$$\gamma_k(G) \triangleq \frac{\lambda_2}{1 - (4/k) \cdot \theta_k(G)}.$$

Our next theorem shows that the structure of clusters in G and the eigenvector corresponding to $\lambda_1(\mathcal{L}_G)$ can be approximated by each other with approximation ratio inversely proportional to $\gamma_k(G)$.

Theorem 3.2. *The following statements hold: (1) there is some $\alpha \in \mathbb{C}$ such that the vector $\tilde{f}_1 = \alpha f_1$ satisfies $\|y - \tilde{f}_1\|^2 \leq 1/\gamma_k(G)$; (2) there is some $\beta \in \mathbb{C}$ such that the vector $\tilde{y} = \beta y$ satisfies $\|f_1 - \tilde{y}\|^2 \leq 1/(\gamma_k(G) - 1)$.*

4 Algorithm

In this section we discuss the algorithmic contribution of the paper. In Section 4.1 we will describe the main algorithm, and its efficient implementation based on nearly-linear time Laplacian solvers; we will further present a sub-linear time implementation of our algorithm, assuming the degrees of the vertices are known in advance. The main technical ideas used in analysing the algorithms will be discussed in Section 4.2.

4.1 Algorithm Description

Main algorithm. We have seen from Section 3 that the structure of clusters is approximately encoded in the bottom eigenvector of \mathcal{L}_G . To exploit this fact, we propose to embed the vertices of G into \mathbb{R}^2 based on the bottom eigenvector of \mathcal{L}_G , and apply k -means on the embedded points. Our algorithm, which we call `SimpleHerm`, only consists of a few lines of code and is described as follows: (1) compute the bottom eigenvector $f_1 \in \mathbb{C}^n$ of the normalised Hermitian Laplacian matrix \mathcal{L}_G of G ; (2) compute the embedding $\{F(v)\}_{v \in V[G]}$, where $F(v) \triangleq \frac{1}{\sqrt{d_v}} \cdot f_1(v)$ for any vertex v ; (3) apply k -means on the embedded points $\{F(v)\}_{v \in V[G]}$.

We remark that, although the entries of \mathcal{L}_G are complex-valued, some variant of the graph Laplacian solvers could still be applied for our setting. For most practical instances, we have $k = O(\log^c n)$ for some constant c , in which regime our proposed algorithm runs in nearly-linear time³. We refer a reader to [22] on technical discussion on the algorithm of approximating f_1 in nearly-linear time.

Speeding-up the runtime of the algorithm. Since $\Omega(m)$ time is needed for any algorithm to read an entire graph, the runtime of our proposed algorithm is optimal up to a poly-logarithmic factor. However we will show that, when the vertices' degrees are available in advance, the following sub-linear time algorithm could be applied before the execution of the main algorithm, and this will result in the algorithm's total runtime to be sub-linear in m .

More formally, our proposed sub-linear time implementation is to construct a sparse subgraph H of the original input graph G , and run the main algorithm on H instead. The algorithm for obtaining graph H works as follows: every vertex u in the graph G checks each of its outgoing edges $e = (u, v)$, and samples each outgoing edge with probability

$$p_u(u, v) \triangleq \min \left\{ w(u, v) \cdot \frac{\alpha \cdot \log n}{\lambda_2 \cdot d_u^{\text{out}}}, 1 \right\};$$

in the same time, every vertex v checks each of its incoming edges $e = (u, v)$ with probability

$$p_v(u, v) \triangleq \min \left\{ w(u, v) \cdot \frac{\alpha \cdot \log n}{\lambda_2 \cdot d_v^{\text{in}}}, 1 \right\},$$

where $\alpha \in \mathbb{R}_{>0}$ is some constant which can be determined experimentally. As the algorithm goes through each vertex, it maintains all the sampled edges in a set F . Once all the edges have

³Given any graph G with n vertices and m edges as input, we say an algorithm runs in nearly-linear time if the algorithm's runtime is $O(m \cdot \log^c n)$ for some constant c .

been checked, the algorithm returns a weighted graph $H = (V, F, w_H)$, where each sampled edge $e = (u, v)$ has a new weight defined by $w_H(u, v) = w(u, v)/p_e$. Here, p_e is the probability that e is sampled by one of its endpoints and, for any $e = (u, v)$, we can write p_e as $p_e = p_u(u, v) + p_v(u, v) - p_u(u, v)p_v(u, v)$.

4.2 Analysis

Analysis of the main algorithm. Now we analyse the proposed algorithm, and prove that running k -means on $\{F(v)\}_{v \in V[G]}$ is sufficient to obtain a meaningful clustering with bounded approximation guarantee. We assume that the output of a k -means algorithm is A_0, \dots, A_{k-1} . We define the cost function of the output clustering A_0, \dots, A_{k-1} by

$$\text{COST}(A_0, \dots, A_{k-1}) \triangleq \min_{c_0, \dots, c_{k-1} \in \mathbb{C}} \sum_{j=0}^{k-1} \sum_{u \in A_j} d_u \|F(u) - c_j\|^2,$$

and define the optimal clustering by

$$\Delta_k^2 \triangleq \min_{\text{partition } A_0, \dots, A_{k-1}} \text{COST}(A_0, \dots, A_{k-1}).$$

Although computing the optimal clustering for k -means is NP-hard, we will show that the cost value for the optimal clustering can be upper bounded with respect to $\gamma_k(G)$. To achieve this, we define k points $p^{(0)}, \dots, p^{(k-1)}$ in \mathbb{C} , where $p^{(j)}$ is defined by

$$p^{(j)} = \frac{\beta}{\sqrt{k}} \cdot \frac{(\omega_{\lceil 2\pi \cdot k \rceil})^j}{\sqrt{\text{vol}(S_j)}}, \quad 0 \leq j \leq k-1. \quad (4)$$

We could view these $p^{(0)}, \dots, p^{(k-1)}$ as approximate centers of the k clusters, which are separated from each other through different powers of $\omega_{\lceil 2\pi \cdot k \rceil}$.

Our first lemma shows that the total distance between the embedded points from every S_j and their respective centers $p^{(j)}$ can be upper bounded, which is summarised as follows:

Lemma 4.1. *It holds that $\sum_{j=0}^{k-1} \sum_{u \in S_j} d_u \cdot \|F(u) - p^{(j)}\|^2 \leq (\gamma_k(G) - 1)^{-1}$.*

Since the cost value of the optimal clustering is the minimum over all possible partitions of the embedded points, by Lemma 4.1 we have that $\Delta_k^2 \leq (\gamma_k(G) - 1)^{-1}$. We assume that the k -means algorithm used here achieves an approximation ratio of APT. Therefore, the output A_0, \dots, A_{k-1} of this k -means algorithm satisfies $\text{COST}(A_0, \dots, A_{k-1}) \leq \text{APT}/(\gamma_k(G) - 1)$.

Secondly, we show that the norm of the approximate centre of each cluster is *inversely* proportional to the volume of each cluster. This implies that larger clusters are closer to the origin, while smaller clusters are further away from the origin.

Lemma 4.2. *It holds for any $0 \leq j \leq k-1$ that $\|p^{(j)}\|^2 = \|\beta\|^2 \cdot (k \cdot \text{vol}(S_j))^{-1}$.*

Thirdly, we prove that the distance between different approximate centres $p^{(j)}$ and $p^{(\ell)}$ is inversely proportional to the volume of the *smaller* cluster, which implies that the embedded points of the vertices from a smaller cluster are far from the embedded points from other clusters. This key fact explains why our algorithm is able to approximately recover the structure of all the clusters.

Lemma 4.3. *It holds for any $0 \leq j \neq \ell \leq k-1$ that $\|p^{(j)} - p^{(\ell)}\|^2 \geq \frac{\|\beta\|^2}{3k^3 \cdot \min\{\text{vol}(S_j), \text{vol}(S_\ell)\}}$.*

Combining these three lemmas with some combinatorial analysis, we prove that the symmetric difference between every returned cluster by the algorithm and its corresponding cluster in the optimal partition can be upper bounded, since otherwise the cost value of the returned clusters would contradict Lemma 4.1.

Theorem 4.4. *Let $G = (V, E)$ be a digraph, and S_0, \dots, S_{k-1} be a k -way partition of $V[G]$ that maximises the flow ratio $\Phi_G(S_0, \dots, S_{k-1})$. Then, there is an algorithm that returns a k -way partition A_0, \dots, A_{k-1} of $V[G]$. Moreover, by assuming A_j corresponds to S_j in the optimal partition, it holds that $\text{vol}(A_j \triangle S_j) \leq \varepsilon \text{vol}(S_j)$ for some $\varepsilon = 48k^3 \cdot (1 + \text{APT}) / (\gamma_k(G) - 1) \leq 1/2$.*

We remark that the analysis of our algorithm is similar with the work of [23]. However, the analysis in [23] relies on k indicator vectors of k clusters, each of which is in a different dimension of \mathbb{R}^n ; this implies that k eigenvectors are needed in order to find a good k -way partition. In our case, all the embedded points are in \mathbb{R}^2 , and the embedded points from different clusters are mainly separated by angles; this makes our analysis slightly more involved than [23].

Analysis for the speeding-up subroutine. We further analyse the speeding-up subroutine described in Section 4.1. Our analysis is very similar with [27], and the approximation guarantee of our speeding-up subroutine is as follows:

Theorem 4.5. *Given a digraph $G = (V, E)$ as input, the speeding-up subroutine computes a subgraph $H = (V, F)$ of G with $O((1/\lambda_2) \cdot n \log n)$ edges. Moreover, with high probability, the computed sparse graph H satisfies that $\theta_k(H) = \Omega(\theta_k(G))$, and $\lambda_2(\mathcal{L}_H) = \Omega(\lambda_2(\mathcal{L}_G))$.*

5 Experiments

In this section we present the experimental results of our proposed algorithm SimpleHerm on both synthetic and real-world datasets, and compare its performance against the previous state-of-the-art. All our experiments are conducted with an ASUS ZenBook Pro UX501VW with an Intel(R) Core(TM) i7-6700HQ CPU @ 2.60GHz with 12GB of RAM.

We will compare SimpleHerm against the DD-SYM algorithm [24] and the Herm-RW algorithm [9]. Given the adjacency matrix $M \in \mathbb{R}^{n \times n}$ as input, the DD-SYM algorithm computes the matrix $A = M^\top M + MM^\top$, and uses the top k eigenvectors of a random walk matrix $D^{-1}A$ to construct an embedding for k -means clustering. The Herm-RW algorithm uses the imaginary unit i to represent directed edges and applies the top $\lceil k/2 \rceil$ eigenvectors of a random walk matrix to construct an embedding for k -means. Notice that both of the DD-SYM and Herm-RW algorithms involve the use of multiple eigenvectors, and DD-SYM requires computing matrix multiplications, which makes it computationally more expensive than ours.

5.1 Results on Synthetic Datasets

We first perform experiments on graphs generated from the Directed Stochastic Block Model (DSBM) which is introduced in [9]. We introduce a path structure into the DSBM, and compare the performance of our algorithm against the others. Specifically, for given parameters k, n, p, q, η , a graph randomly chosen from the DSBM is constructed as follows: the overall graph consists of k clusters S_0, \dots, S_{k-1} of the same size, each of which can be initially viewed as a $G(n, p)$ random graph. We connect edges with endpoints in different clusters with probability q , and connect edges with endpoints within the same cluster with probability p . In addition, for any edge (u, v) where $u \in S_j$ and $v \in S_{j+1}$, we set the edge direction as $u \rightsquigarrow v$ with probability η , and set the edge direction as $v \rightsquigarrow u$ with probability $1 - \eta$. For all other pairs of clusters which do not lie along the path, we set their edge directions randomly. The directions of edges inside a cluster are assigned randomly.

As graphs generated from the DSBM have a well-defined ground truth clustering, we apply the Adjusted Rand Index (ARI) [14] to measure the performance of different algorithms. We further set $p = q$, since this is one of the hardest regimes for studying the DSBM. In particular, when $p = q$, the edge density plays no role in characterising the structure of clusters, and the edges are *entirely* defined with respect to the edge directions.

We set $n = 1000$, and $k = 4$. We set the value of p to be between 0.5 and 0.8, and the value of η to be between 0.5 and 0.7. As shown in Figure 1, our proposed SimpleHerm clearly outperforms the Herm-RW and the DD-SYM algorithms.

Next, we study the case of $n = 2000$ and $k = 8$, but the structure of clusters presents a more significant path topology. Specifically, we assume that any pair of vertices within each cluster are connected with probability $p \in (0.05, 0.1)$; moreover, all the edges crossing different clusters are along the cuts (S_j, S_{j+1}) for some $0 \leq j \leq k - 2$. By setting $\eta \in (0.65, 1)$, our results are reported in Figure 2. From these results, it is easy to see that, when the underlying graph presents a clear flow structure, our algorithm performs significantly better than both the Herm-RW and DD-SYM algorithms, for which multiple eigenvectors are needed.

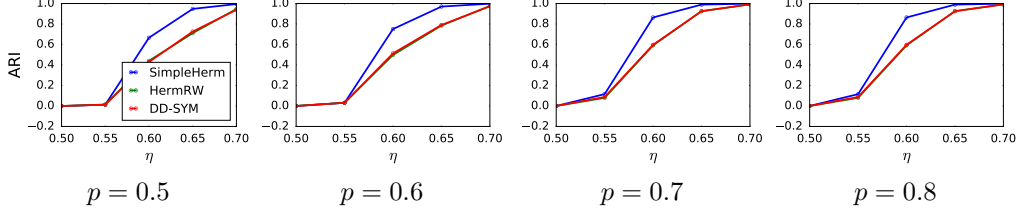


Figure 1: $n = 1000$ and $k = 4$. Average ARIs over 5 runs of different algorithms, with respect to different values of p and η .

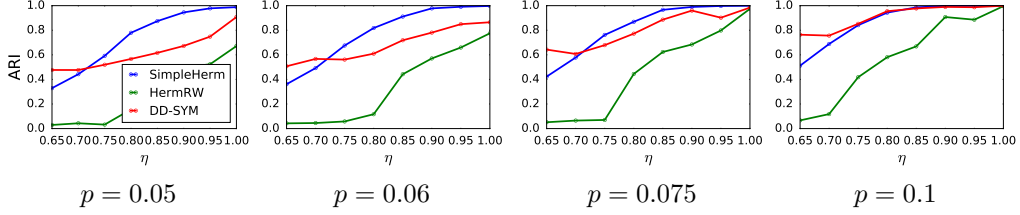


Figure 2: $n = 2000$ and $k = 8$. Average ARIs over 5 runs of different algorithms, with respect to different values of p and η .

5.2 Results on the UN Comtrade Dataset

We compare our proposed algorithm against the previous state-of-the-art on the UN Comtrade Dataset [29]. This dataset consists of the import-export trade flow data of 97 specific commodities across $N = 246$ countries and territories over the period 1964 – 2018. The total size of the data in zipped files is 99.8GB, where every csv file for a single year contained around 20,000,000 lines.

Pre-processing. As the pre-processing step, for any fixed commodity c and any fixed year, we construct a directed graph as follows: the constructed graph has $N = 246$ vertices, which correspond to 246 countries and territories listed in the dataset. For any two vertices j and ℓ , there is a directed edge from j to ℓ if the export of commodity c from country j to ℓ is greater than the export from ℓ to j , and the weight of that edge is set to be the absolute value of the difference in trade, i.e., the net trade value between ℓ and j . Notice that our construction ensures that all the edge weights are non-negative, and there is at most one directed edge between any pair of vertices.

Result on the International Oil Trade Industry. We first study the international trade for mineral fuels, oils, and oil distillation product in the dataset. The primary reason for us to study the international oil trade is due to the fact that crude oil is one of the highest traded commodities worldwide [2], and plays a significant role in geopolitics (e.g., 2003 Iraq War). Many references in international trade and policy making (e.g., [3, 10, 11]) allow us to interpret the results of our proposed algorithm.

Following previous studies on the same dataset from complex networks’ perspectives [13, 32], we set $k = 4$. Our algorithm’s output around the period of 2006–2009 is visualised in Figure 3. We choose to highlight the results between 2006 and 2009, since 2008 sees the largest post World War II oil shock after the economic crisis [18]. As discussed earlier, our algorithm’s output is naturally associated with an ordering of the clusters that optimises the value of Φ , and this ordering is reflected in our visualisation as well. Notice that such ordering corresponds to the chain of oil trade, and indicates the clusters of main export countries and import countries for oil trade.

From Figure 3, we see that the output of our algorithm from 2006 to 2008 is pretty stable, and this is in sharp contrast to the drastic change between 2008 and 2009, caused by the economic crisis. Moreover, many European countries move across different clusters from 2008 to 2009. The visualisation results of the other algorithms are less significant than ours.

We further show that this dynamic change of clusters provides a reasonable reflection of international economics. Specifically, we compute the clustering results of our SimpleHerm algorithm on the same dataset from 2002 to 2017, and compare it with the output of the DD-SYM algorithm. For every two

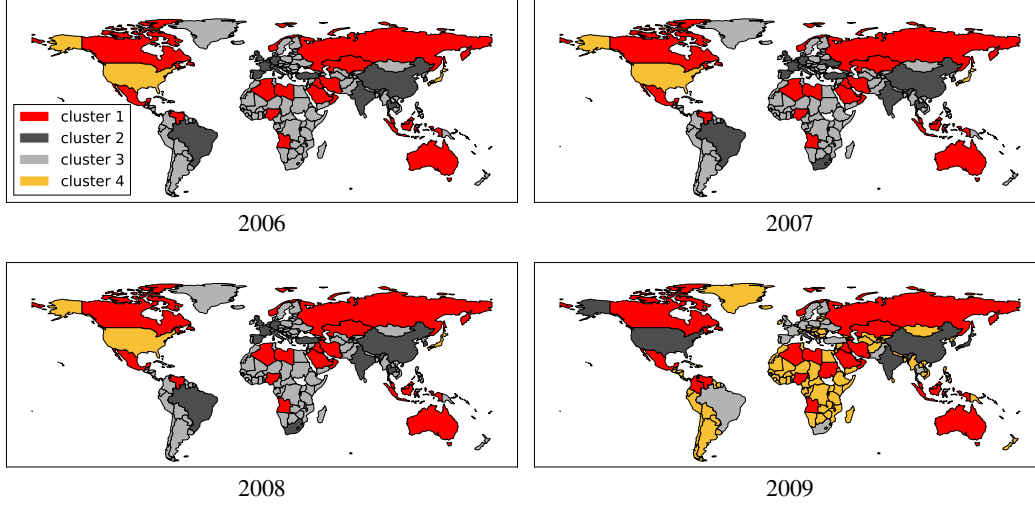


Figure 3: The clustering result for international trade from 2006 to 2009, where $k = 4$. Red countries form start of the trade chain, and yellow countries the end of the trade chain. Countries coloured white have no data.

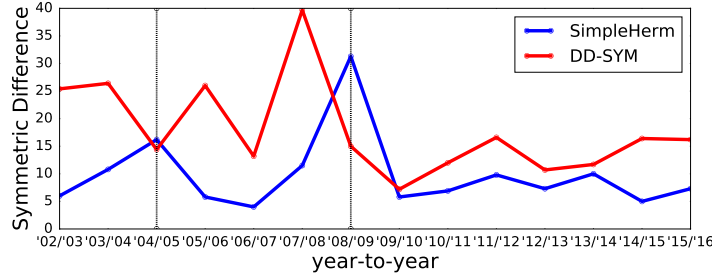


Figure 4: Comparison of the symmetric difference of the returned clusters between two consecutive years.

consecutive years, we map every cluster to its “optimal” correspondence (i.e., the one that minimises the symmetric difference between the two). We further compute the total symmetric difference between the clustering results for every two consecutive years, and our results are visualised in Figure 4. As shown in the figure, our algorithm has notable changes in clustering during 2004/2005 and 2008/2009 respectively. The peak around 2004/2005 might be a delayed change as a consequence of the Venezuelan oil strike and the Iraq war of 2003. Both the events led to the decrease in oil barrel production by 5.4 million barrels per day [16]. The peak around 2008/2009 is of course due to the economic crisis. These peaks correspond to the same periods of cluster instability found in the complex network analysis literature [1, 33], further signifying our result⁴. Compared to our algorithm, the clustering result of the DD-SYM algorithm is less stable over time.

Result on the International Wood Trade. We also study the international wood trade network (IWTN). This network looks at the trade of wood and articles of wood. Although the IWTN is less studied than the International Oil Trade Industry in the literature, it is nonetheless the reflection of an important and traditional industry and deserves detailed analysis. Wood trade is dependent on a number of factors, such as the amount of forest a country has left, whether countries are trying to reintroduce forests, and whether countries are deforesting a lot for agriculture (e.g., Amazon rainforest in Brazil) [17].

⁴We didn’t plot the result between 2016 and 2017, since the symmetric difference for the DD-SYM algorithm is 107 and the symmetric difference for the SimpleHerm algorithm is 17. We believe this is an anomaly for DD-SYM, and plotting this result in the same figure would make it difficult to compare other years’ results.

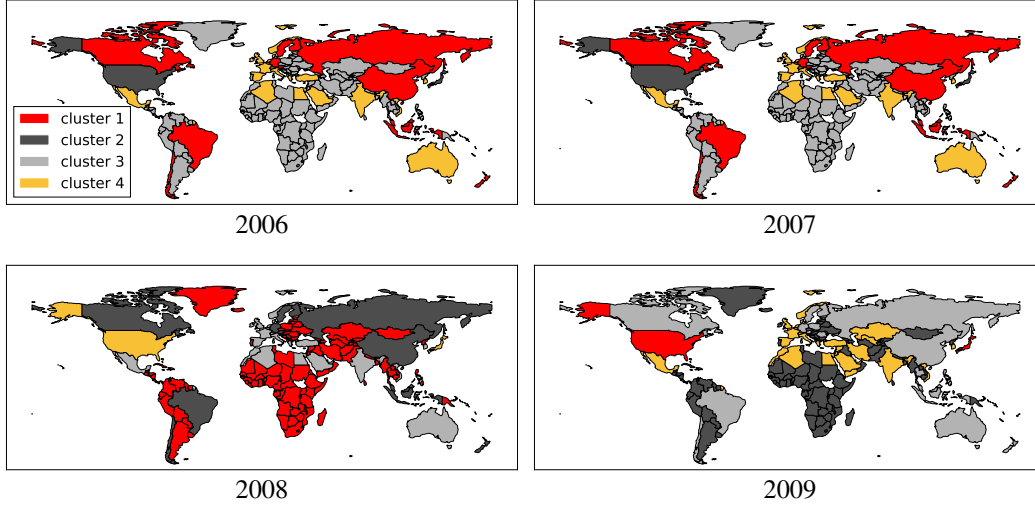


Figure 5: Change in clustering of SimpleHerm of the IWTN from 2006 to 2009 with $k = 4$. Clusters are labelled according to their position in the ordering that maximises the flow ratio between the 4 clusters. Red countries form start of the trade chain, and yellow countries the end of the trade chain. Countries coloured in white have no data.

Figure 5 visualises the clusters from 2006 to 2009. As we can see, the structure of clusters are stable in early years, and the first cluster contains countries with large forests such as Canada, Brazil, Russia, Germany, and China. However, there is a significant change of the cluster structure from 2008 to 2009, and countries in Eastern Europe, the Middle East and Central Asia move across different clusters.

5.3 Result on the Data Science for COVID-19 Dataset

The Data Science for COVID-19 Dataset (DS4C) [19] contains information about 3519 South Korean citizens infected with COVID-19. Here, digraphs are essential to represent how the virus is transmitted among the individuals, and the clusters with high ratio of out-going edges represent the communities worst hit by the virus. We first identify the largest connected component of the infection graph, which consists of 67 vertices and 66 edges, and run our algorithm on the largest connected component. By setting $k = 4$, our algorithm manages to identify a super-spreader as a single cluster, and the path of infection between groups of people along which most infections lie.

6 Broader Impact

The primary focus of our work is efficient clustering algorithms for digraphs, whose clusters are defined with respect to the edge directions between different clusters. We believe that our work could have long-term social impact. For instance, when modelling the transmission of COVID-19 among individuals through a digraph, the cluster (group of people) with the highest ratio of out-going edges represents the most infectious community. This type of information could aid local containment policy. With the development of many tracing Apps for COVID-19 and a significant amount of infection data available in the near future, our studied algorithm could potentially be applied in this context. In addition, as shown by our experimental results on the UN Comtrade Dataset, our work could be employed to analyse many practical data for which most traditional clustering algorithms do not suffice.

Acknowledgments and Disclosure of Funding

Part of this work was done when Steinar Laenen studied at the University of Edinburgh as a Master student. He Sun is supported by an EPSRC Early Career Fellowship (EP/T00729X/1).

References

- [1] H. An, W. Zhong, Y. Chen, H. Li, and X. Gao. Features and evolution of international crude oil trade relationships: A trading-based network analysis. *Energy*, 74:254 – 259, 2014.
- [2] F. I. Association. Total 2017 volume 25.2 billion contracts, down 0.1% from 2016. <https://www.fia.org/resources/total-2017-volume-252-billion-contracts-down-01-2016>, Jan 2018. Accessed: 2020-06-05.
- [3] N. B. Behmiri and J. R. P. Manso. Crude oil conservation policy hypothesis in OECD (organisation for economic cooperation and development) countries: A multivariate panel Granger causality test. *Energy*, 43(1):253–260, 2012.
- [4] A. R. Benson, D. F. Gleich, and J. Leskovec. Tensor spectral clustering for partitioning higher-order network structures. In *International Conference on Data Mining*, pages 118–126, 2015.
- [5] A. R. Benson, D. F. Gleich, and J. Leskovec. Higher-order organization of complex networks. *Science*, 353(6295):163–166, 2016.
- [6] F. Chung. Spectral graph theory. In *CBMS: Conference Board of the Mathematical Sciences, Regional Conference Series*, 1997.
- [7] F. Chung. Laplacians and the Cheeger inequality for directed graphs. *Annals of Combinatorics*, 9(1):1–19, 2005.
- [8] F. Chung and L. Lu. Concentration inequalities and martingale inequalities: a survey. *Internet Mathematics*, 3(1):79–127, 2006.
- [9] M. Cucuringu, H. Li, H. Sun, and L. Zanetti. Hermitian matrices for clustering directed graphs: insights and applications. In *International Conference on Artificial Intelligence and Statistics*, 2020.
- [10] L.-B. Cui, P. Peng, and L. Zhu. Embodied energy, export policy adjustment and China’s sustainable development: a multi-regional input-output analysis. *Energy*, 82:457–467, 2015.
- [11] N. Cui, Y. Lei, and W. Fang. Design and impact estimation of a reform program of China’s tax and fee policies for low-grade oil and gas resources. *Petroleum Science*, 8(4):515–526, 2011.
- [12] M. Dittrich and S. Bringezu. The physical dimension of international trade: Part 1: Direct global flows between 1962 and 2005. *Ecological Economics*, 69(9):1838 – 1847, 2010.
- [13] R. Du, G. Dong, L. Tian, M. Wang, G. Fang, and S. Shao. Spatiotemporal dynamics and fitness analysis of global oil market: Based on complex network. *Public Library of Science one*, 11(10), 2016.
- [14] A. J. Gates and Y.-Y. Ahn. The impact of random models on clustering similarity. *The Journal of Machine Learning Research*, 18(1):3049–3076, 2017.
- [15] M. X. Goemans and D. P. Williamson. Improved approximation algorithms for maximum cut and satisfiability problems using semidefinite programming. *Journal of the ACM*, 42(6):1115–1145, 1995.
- [16] J. D. Hamilton. Historical oil shocks. Technical report, National Bureau of Economic Research, 2011.
- [17] T. Kastner, K.-H. Erb, and S. Nonhebel. International wood trade and forest change: A global analysis. *Global Environmental Change*, 21(3):947–956, 2011.
- [18] L. Kilian. Exogenous oil supply shocks: how big are they and how much do they matter for the US economy? *The Review of Economics and Statistics*, 90(2):216–240, 2008.
- [19] Korea Centers for Disease Control & Prevention. Data science for COVID-19. <https://www.kaggle.com/kimjihoo/coronavirusdataset>, 2020. Accessed: 2020-06-03.
- [20] J. R. Lee, S. O. Gharan, and L. Trevisan. Multiway spectral partitioning and higher-order Cheeger inequalities. *Journal of the ACM*, 61(6):37:1–37:30, 2014.
- [21] E. A. Leicht and M. E. J. Newman. Community structure in directed networks. *Physical Review Letters*, 100:118703, 2008.
- [22] H. Li, H. Sun, and L. Zanetti. Hermitian Laplacians and a Cheeger inequality for the Max-2-Lin problem. In *27th Annual European Symposium on Algorithms (ESA)*, pages 1–14, 2019.
- [23] R. Peng, H. Sun, and L. Zanetti. Partitioning well-clustered graphs: Spectral clustering works! *SIAM J. Comput.*, 46(2):710–743, 2017.
- [24] V. Satuluri and S. Parthasarathy. Symmetrizations for clustering directed graphs. In *Proceedings of the 14th International Conference on Extending Database Technology*, pages 343–354, 2011.
- [25] J. Shi and J. Malik. Normalized cuts and image segmentation. In *Conference on Computer Vision and Pattern Recognition (CVPR)*, pages 731–737, 1997.
- [26] D. A. Spielman and N. Srivastava. Graph sparsification by effective resistances. *SIAM Journal on Computing*, 40(6):1913–1926, 2011.

- [27] H. Sun and L. Zanetti. Distributed graph clustering and sparsification. *ACM Transactions on Parallel Computing*, 6(3):17:1–17:23, 2019.
- [28] J. A. Tropp. User-friendly tail bounds for sums of random matrices. *Foundations of computational mathematics*, 12(4):389–434, 2012.
- [29] United Nations. UN comtrade free API. <https://comtrade.un.org/data/>. Accessed: 2020-06-03.
- [30] U. Von Luxburg. A tutorial on spectral clustering. *Statistics and computing*, 17(4):395–416, 2007.
- [31] H. Yin, A. R. Benson, J. Leskovec, and D. F. Gleich. Local higher-order graph clustering. In *23rd International Conference on Knowledge Discovery and Data Mining (SIGKDD)*, pages 555–564, 2017.
- [32] Z. Zhang, H. Lan, and W. Xing. Global trade pattern of crude oil and petroleum products: Analysis based on complex network. In *IOP Conference Series: Earth and Environmental Science*, volume 153, pages 22–33. IOP Publishing, 2018.
- [33] W. Zhong, H. An, X. Gao, and X. Sun. The evolution of communities in the international oil trade network. *Physica A: Statistical Mechanics and its Applications*, 413:42 – 52, 2014.

A Omitted details from Section 3

In this section we present all the technical detailed omitted from Section 3.

Proof of Lemma 3.1. We prove the statement by analysing the Reyleigh quotient of \mathcal{L}_G with respect to y , which is defined by $\frac{y^* \mathcal{L}_G y}{y^* y}$. Since $\|y\| = 1$, it suffices to analyse $y^* \mathcal{L}_G y$. By definition, we have that

$$\begin{aligned}
 y^* \mathcal{L}_G y &= \frac{1}{k} \left(\sum_{j=0}^{k-1} \widehat{\chi}_j \right)^* \mathcal{L}_G \left(\sum_{j=0}^{k-1} \widehat{\chi}_j \right) \\
 &= \frac{1}{k} \left(\sum_{j=0}^{k-1} \frac{D^{1/2} \chi_j}{\|D^{1/2} \chi_j\|} \right)^* D^{-1/2} (D - A) D^{-1/2} \left(\sum_{j=0}^{k-1} \frac{D^{1/2} \chi_j}{\|D^{1/2} \chi_j\|} \right) \\
 &= \frac{1}{k} \left(\sum_{j=0}^{k-1} \frac{\chi_j}{\|D^{1/2} \chi_j\|} \right)^* (D - A) \left(\sum_{j=0}^{k-1} \frac{\chi_j}{\|D^{1/2} \chi_j\|} \right). \tag{5}
 \end{aligned}$$

To analyse (5), first of all it is easy to see that

$$\begin{aligned}
 \frac{1}{k} \left(\sum_{j=0}^{k-1} \frac{\chi_j}{\|D^{1/2} \chi_j\|} \right)^* D \left(\sum_{j=0}^{k-1} \frac{\chi_j}{\|D^{1/2} \chi_j\|} \right) &= \frac{1}{k} \left(\sum_{j=0}^{k-1} \frac{\chi_j}{\|D^{1/2} \chi_j\|} \right)^* D^{1/2} D^{1/2} \left(\sum_{j=0}^{k-1} \frac{\chi_j}{\|D^{1/2} \chi_j\|} \right) \\
 &= \frac{1}{k} \left(\sum_{j=0}^{k-1} \frac{D^{1/2} \chi_j}{\|D^{1/2} \chi_j\|} \right)^* \left(\sum_{j=0}^{k-1} \frac{D^{1/2} \chi_j}{\|D^{1/2} \chi_j\|} \right) \\
 &= \frac{1}{k} \sum_{j=0}^{k-1} \frac{\chi_j^* D \chi_j}{\|D^{1/2} \chi_j\|^2} \\
 &= 1, \tag{6}
 \end{aligned}$$

where the third equality follows by the fact that $\chi_j^* \chi_\ell = 0$ for any $0 \leq j \neq \ell \leq k-1$. On the other hand, by definition we have that

$$\begin{aligned}
& \frac{1}{k} \left(\sum_{j=0}^{k-1} \frac{\chi_j}{\|D^{1/2} \chi_j\|} \right)^* A \left(\sum_{j=0}^{k-1} \frac{\chi_j}{\|D^{1/2} \chi_j\|} \right) \\
&= \frac{1}{k} \left(\sum_{j=0}^{k-1} \frac{\chi_j}{\sqrt{\text{vol}(S_j)}} \right)^* A \left(\sum_{j=0}^{k-1} \frac{\chi_j}{\sqrt{\text{vol}(S_j)}} \right) \\
&= \frac{1}{k} \cdot \sum_{j=0}^{k-1} \sum_{\ell=0}^{k-1} \sum_{\substack{u \rightsquigarrow v \\ u \in S_j, v \in S_\ell}} \left(\frac{\overline{\chi_j}(u)}{\sqrt{\text{vol}(S_j)}} \cdot A_{u,v} \cdot \frac{\chi_\ell(v)}{\sqrt{\text{vol}(S_\ell)}} + \frac{\overline{\chi_\ell}(v)}{\sqrt{\text{vol}(S_\ell)}} \cdot A_{v,u} \cdot \frac{\chi_j(u)}{\sqrt{\text{vol}(S_j)}} \right) \\
&= \frac{1}{k} \cdot \sum_{j=0}^{k-1} \sum_{\ell=0}^{k-1} \sum_{\substack{u \rightsquigarrow v \\ u \in S_j, v \in S_\ell}} \frac{w(u, v)}{\sqrt{\text{vol}(S_j)} \cdot \sqrt{\text{vol}(S_\ell)}} \cdot 2 \cdot \text{Re} \left((\omega_{\lceil 2\pi \cdot k \rceil})^{\ell+1-j} \right) \\
&= \frac{1}{k} \cdot \sum_{j=0}^{k-1} \sum_{\ell=0}^{k-1} \frac{w(S_j, S_\ell)}{\sqrt{\text{vol}(S_j)} \cdot \sqrt{\text{vol}(S_\ell)}} \cdot 2 \cdot \cos \left(\frac{2\pi \cdot (\ell+1-j)}{\lceil 2\pi \cdot k \rceil} \right), \tag{7}
\end{aligned}$$

where $\text{Re}(\cdot)$ stands for the real part of a complex number. Combining (5), (6) with (7), we have that

$$\begin{aligned}
& y^* \mathcal{L}_G y \\
&= 1 - \frac{1}{k} \cdot \sum_{j=0}^{k-1} \sum_{\ell=0}^{k-1} \frac{w(S_j, S_\ell)}{\sqrt{\text{vol}(S_j)} \cdot \sqrt{\text{vol}(S_\ell)}} \cdot 2 \cdot \cos \left(\frac{2\pi \cdot (\ell+1-j)}{\lceil 2\pi \cdot k \rceil} \right) \\
&\leq 1 - \frac{1}{k} \cdot \sum_{j=0}^{k-1} \sum_{\ell=0}^{k-1} \frac{w(S_j, S_\ell)}{\sqrt{\text{vol}(S_j)} \sqrt{\text{vol}(S_\ell)}} \cdot \left(2 - \left(\frac{2\pi \cdot (\ell+1-j)}{\lceil 2\pi \cdot k \rceil} \right)^2 \right) \\
&\leq 1 - \frac{1}{k} \cdot \sum_{j=0}^{k-1} \sum_{\ell=0}^{k-1} \frac{2 \cdot w(S_j, S_\ell)}{\sqrt{\text{vol}(S_j)} \sqrt{\text{vol}(S_\ell)}} + \frac{1}{k} \cdot \sum_{j=0}^{k-1} \sum_{\ell=0}^{k-1} \frac{w(S_j, S_\ell)}{\sqrt{\text{vol}(S_j)} \sqrt{\text{vol}(S_\ell)}} \left(\frac{\ell+1-j}{k} \right)^2 \\
&\leq 1 - \frac{1}{k} \cdot \sum_{j=0}^{k-1} \sum_{\substack{\ell=0 \leq \ell \leq k-1 \\ \ell \neq j-1}} \frac{2 \cdot w(S_j, S_\ell)}{\sqrt{\text{vol}(S_j)} \sqrt{\text{vol}(S_\ell)}} + \frac{1}{k} \cdot \sum_{j=0}^{k-1} \sum_{\substack{\ell=0 \leq \ell \leq k-1 \\ \ell \neq j-1}} \frac{2 \cdot w(S_j, S_\ell)}{\sqrt{\text{vol}(S_j)} \sqrt{\text{vol}(S_\ell)}} \left(\frac{\ell+1-j}{k} \right)^2 \\
&= 1 - \frac{1}{k} \cdot \sum_{j=0}^{k-1} \sum_{\substack{\ell=0 \leq \ell \leq k-1 \\ \ell \neq j-1}} \frac{2 \cdot w(S_j, S_\ell)}{\sqrt{\text{vol}(S_j)} \sqrt{\text{vol}(S_\ell)}} \left(1 - \left(\frac{\ell+1-j}{k} \right)^2 \right) - \frac{1}{k} \cdot \sum_{j=1}^{k-1} \frac{2 \cdot w(S_j, S_{j-1})}{\sqrt{\text{vol}(S_j)} \sqrt{\text{vol}(S_{j-1})}} \\
&\leq 1 - \frac{1}{k} \cdot \sum_{j=1}^{k-1} \frac{2 \cdot w(S_j, S_{j-1})}{\sqrt{\text{vol}(S_j)} \sqrt{\text{vol}(S_{j-1})}} \\
&= 1 - \frac{2}{k} \cdot \sum_{j=1}^{k-1} \frac{w(S_j, S_{j-1})}{\sqrt{\text{vol}(S_j)} \sqrt{\text{vol}(S_{j-1})}} \\
&\leq 1 - \frac{4}{k} \cdot \sum_{j=1}^{k-1} \frac{w(S_j, S_{j-1})}{\text{vol}(S_j) + \text{vol}(S_{j-1})} \\
&= 1 - \frac{4}{k} \cdot \theta_k(G),
\end{aligned}$$

where the first inequality follows by the fact that $\cos x \geq 1 - x^2/2$ and the last inequality follows by the inequality $2ab \leq a^2 + b^2$ for any $a, b \in \mathbb{R}$. Therefore, we have that

$$\frac{y^* \mathcal{L}_G y}{y^* y} \leq 1 - \frac{4}{k} \cdot \theta_k(G).$$

By the Rayleigh characterisation of eigenvalues we know that

$$\lambda_1(\mathcal{L}_G) = \min_{x \in \mathbb{C}^n \setminus \{0\}} \frac{x^* \mathcal{L}_G x}{x^* x} \leq 1 - \frac{4}{k} \cdot \theta_k(G),$$

which proves the first statement of the lemma.

Now we prove the second statement. Let G be a digraph, and S_0, \dots, S_{k-1} be the k clusters maximising $\Phi_G(S_0, \dots, S_{k-1})$, i.e., $\Phi_G(S_0, \dots, S_{k-1}) = \theta_k(G)$. Since adding edges that are not along the path only decreases the value of Φ_G , we assume without loss of generality that all the edges are along the path. For the base case of $k = 2$, we have that

$$\Phi_G(S_0, S_1) = \frac{w(S_0, S_1)}{\text{vol}(S_0) + \text{vol}(S_1)} = \frac{1}{2} = \frac{k}{4}.$$

Next, we will prove that $\theta_k(G) < k/4$ for any $k \geq 3$. We set $y_j \triangleq w(S_j, S_{j-1})$ for any $1 \leq j \leq k-1$, and have that

$$\begin{aligned} \Phi_G(S_0, \dots, S_{k-1}) &= \sum_{j=1}^{k-1} \frac{w(S_j, S_{j-1})}{\text{vol}(S_j) + \text{vol}(S_{j-1})} \\ &= \frac{y_1}{2y_1 + y_2} + \sum_{j=2}^{k-2} \frac{y_j}{y_{j-1} + 2y_j + y_{j+1}} + \frac{y_{k-1}}{y_{k-2} + 2y_{k-1}}. \end{aligned}$$

By introducing $y_0 = 0$ and assuming that all the indices of $\{y_j\}_j$ are modulo k , we can write $\Phi_G(S_0, \dots, S_{k-1})$ as

$$\Phi_G(S_0, \dots, S_{k-1}) = \sum_{j=0}^{k-1} \frac{y_j}{y_{j-1} + 2y_j + y_{j+1}}.$$

Next we compute $\partial \Phi_G / \partial y_j$, and have that

$$\begin{aligned} \frac{\partial \Phi_G}{\partial y_j} &= \frac{\partial \Phi_G}{\partial y_j} \sum_{j=0}^{k-1} \frac{y_j}{y_{j-1} + 2y_j + y_{j+1}} \\ &= \frac{\partial \Phi_G}{\partial y_j} \left(\frac{y_{j-1}}{y_{j-2} + 2y_{j-1} + y_j} + \frac{y_j}{y_{j-1} + 2y_j + y_{j+1}} + \frac{y_{j+1}}{y_j + 2y_{j+1} + y_{j+2}} \right) \\ &= -\frac{y_{j-1}}{(y_{j-2} + 2y_{j-1} + y_j)^2} + \frac{y_{j-1} + y_{j+1}}{(y_{j-1} + 2y_j + y_{j+1})^2} - \frac{y_{j+1}}{(y_j + 2y_{j+1} + y_{j+2})^2}. \end{aligned}$$

Notice that, when all the y_j ($0 \leq j \leq k-1$) equal to the same non-zero value, it holds that $\partial \Phi_G / \partial y_j = 0$ for any j , and $\theta_k(G) = k/4$. Moreover, it's easy to verify that $k/4$ is an upper bound of θ_k . Since we effectively assume that $y_0 = 0$, which cannot be always equal to all of the y_1, \dots, y_{k-1} , we have that $\theta_k(G) < k/4$. \square

Proof of Theorem 3.2. We first prove the first statement. We write y as a linear combination of the eigenvectors of \mathcal{L}_G by

$$y = \alpha_1 f_1 + \dots + \alpha_n f_n$$

for some $\alpha_i \in \mathbb{C}$ and $f_i \in \mathbb{C}^n$, and define \tilde{f}_1 by $\tilde{f}_1 \triangleq \alpha_1 f_1$. By the definition of the Rayleigh quotient for Hermitian matrices we have that

$$\begin{aligned} \frac{y^* \mathcal{L}_G y}{\|y\|^2} &= (\alpha_1 f_1 + \dots + \alpha_n f_n)^* \mathcal{L}_G (\alpha_1 f_1 + \dots + \alpha_n f_n) \\ &= \|\alpha_1\|^2 \lambda_1(\mathcal{L}_G) + \dots + \|\alpha_n\|^2 \lambda_n(\mathcal{L}_G) \\ &\geq \|\alpha_1\|^2 \lambda_1(\mathcal{L}_G) + (\|\alpha_2\|^2 + \dots + \|\alpha_n\|^2) \lambda_2(\mathcal{L}_G) \\ &\geq (1 - \|\alpha_1\|^2) \lambda_2(\mathcal{L}_G), \end{aligned}$$

where the first inequality holds by the fact that $\lambda_1(\mathcal{L}_G) \leq \dots \leq \lambda_n(\mathcal{L}_G)$ and the second inequality holds by the fact that $\|\alpha_2\|^2 + \dots + \|\alpha_n\|^2 = 1 - \|\alpha_1\|^2$. We can see that

$$\|y - \tilde{f}_1\|^2 = \|\alpha_2\|^2 + \dots + \|\alpha_n\|^2 = 1 - \|\alpha_1\|^2 \leq \frac{1}{\lambda_2} \cdot \frac{y^* \mathcal{L}_G y}{\|y\|} \leq \frac{1}{\gamma_k(G)}.$$

Setting $\alpha = \alpha_1$ proves the first statement.

Next we prove the second statement. By the relationship between f_1 and \tilde{f}_1 , we write

$$f_1 = \beta_1 \tilde{f}_1,$$

where $\beta_1 \triangleq 1/\alpha_1$ is the multiplicative inverse of α_1 . Then, we define \tilde{y} as

$$\tilde{y} = \beta_1 y = \beta_1 (\alpha_1 f_1 + \dots + \alpha_n f_n) = f_1 + \beta_1 (\alpha_2 f_2 + \dots + \alpha_n f_n),$$

and this implies that

$$\begin{aligned} \|f_1 - \tilde{y}\|^2 &= \|\beta_1 (\alpha_2 f_2 + \dots + \alpha_n f_n)\|^2 = \overline{\beta_1} \cdot \left(\sum_{j=2}^n \|\alpha_j\|^2 \right) \cdot \beta_1 = \frac{1}{\|\alpha_1\|^2} (1 - \|\alpha_1\|^2) \\ &\leq \frac{1}{\|\alpha_1\|^2 \cdot \gamma_k(G)}. \end{aligned} \tag{8}$$

Since $1 - \|\alpha_1\|^2 \leq 1/\gamma_k(G)$ implies that

$$\|\alpha_1\|^2 \geq \frac{\gamma_k(G) - 1}{\gamma_k(G)},$$

we can rewrite (8) as

$$\|f_1 - \tilde{y}\|^2 \leq \frac{1}{\gamma_k(G) - 1},$$

and therefore setting $\beta = \beta_1$ proves the second statement. \square

B Omitted details from Section 4

In this section we present all the technical detailed omitted from Section 4.

Proof of Lemma 4.1. By definition, we have that

$$\begin{aligned} \sum_{j=0}^{k-1} \sum_{u \in S_j} d_u \cdot \|F(u) - p^{(j)}\|^2 &= \sum_{j=0}^{k-1} \sum_{u \in S_j} d_u \cdot \left\| \frac{1}{\sqrt{d_u}} \cdot f_1(u) - \frac{\beta}{\sqrt{k}} \cdot \frac{(\omega_{\lceil 2\pi \cdot k \rceil})^j}{\sqrt{\text{vol}(S_j)}} \right\|^2 \\ &= \sum_{j=0}^{k-1} \sum_{u \in S_j} \left\| f_1(u) - \sqrt{\frac{d_u}{k \cdot \text{vol}(S_j)}} \cdot \beta \cdot (\omega_{\lceil 2\pi \cdot k \rceil})^j \right\|^2 \\ &= \sum_{j=0}^{k-1} \sum_{u \in S_j} \|f_1(u) - \tilde{y}(u)\|^2 \\ &= \|f_1 - \tilde{y}\|^2 \\ &\leq \frac{1}{\gamma_k(G) - 1}, \end{aligned}$$

where the last inequality follows by Theorem 3.2. \square

Proof of Lemma 4.2. The proof is by direct calculation on $\|p^{(j)}\|^2$. \square

Proof of Lemma 4.3. By definition of $p^{(j)}$ and $p^{(\ell)}$, we have that

$$\begin{aligned}
& \|p^{(j)} - p^{(\ell)}\|^2 \\
&= \|p^{(j)}\|^2 + \|p^{(\ell)}\|^2 - 2 \cdot \operatorname{Re} \left(p^{(j)} \cdot \overline{p^{(\ell)}} \right) \\
&= \frac{\|\beta\|^2}{k \cdot \operatorname{vol}(S_j)} + \frac{\|\beta\|^2}{k \cdot \operatorname{vol}(S_\ell)} - 2 \cdot \operatorname{Re} \left(\frac{\beta \cdot (\omega_{\lceil 2\pi \cdot k \rceil})^j}{\sqrt{k} \cdot \sqrt{\operatorname{vol}(S_j)}} \cdot \frac{\overline{\beta} \cdot (\omega_{\lceil 2\pi \cdot k \rceil})^{-\ell}}{\sqrt{k} \cdot \sqrt{\operatorname{vol}(S_\ell)}} \right) \\
&= \frac{\|\beta\|^2}{k \cdot \operatorname{vol}(S_j)} + \frac{\|\beta\|^2}{k \cdot \operatorname{vol}(S_\ell)} - 2 \cdot \frac{\|\beta\|^2}{k \cdot \sqrt{\operatorname{vol}(S_j) \cdot \operatorname{vol}(S_\ell)}} \cdot \cos \left(\frac{2\pi \cdot (j - \ell)}{\lceil 2\pi \cdot k \rceil} \right). \tag{9}
\end{aligned}$$

For the case of calculation and the fact that $\cos(x) = \cos(-x)$ for any $x \in \mathbb{R}$, we denote

$$\eta \triangleq \frac{2\pi \cdot |j - \ell|}{\lceil 2\pi \cdot k \rceil},$$

and rewrite (9) as

$$\begin{aligned}
& \|p^{(j)} - p^{(\ell)}\|^2 \\
&= \frac{\|\beta\|^2}{k \cdot \operatorname{vol}(S_j)} + \frac{\|\beta\|^2}{k \cdot \operatorname{vol}(S_\ell)} - 2 \cdot \frac{\|\beta\|^2}{k \cdot \sqrt{\operatorname{vol}(S_j) \cdot \operatorname{vol}(S_\ell)}} \cdot \cos \eta \\
&= \frac{\|\beta\|^2}{k \cdot \max\{\operatorname{vol}(S_j), \operatorname{vol}(S_\ell)\}} + \frac{\|\beta\|^2 \cdot (\sin^2 \eta + \cos^2 \eta)}{k \cdot \min\{\operatorname{vol}(S_j), \operatorname{vol}(S_\ell)\}} - \frac{2 \cos \eta \cdot \|\beta\|^2}{k \cdot \sqrt{\operatorname{vol}(S_j) \cdot \operatorname{vol}(S_\ell)}} \\
&= \left(\frac{\|\beta\|}{\sqrt{k \cdot \max\{\operatorname{vol}(S_j), \operatorname{vol}(S_\ell)\}}} - \frac{\cos \eta \cdot \|\beta\|}{\sqrt{k \cdot \min\{\operatorname{vol}(S_j), \operatorname{vol}(S_\ell)\}}} \right)^2 + \frac{\|\beta\|^2 \cdot \sin^2 \eta}{k \cdot \min\{\operatorname{vol}(S_j), \operatorname{vol}(S_\ell)\}} \\
&\geq \frac{\|\beta\|^2 \cdot \sin^2 \eta}{k \cdot \min\{\operatorname{vol}(S_j), \operatorname{vol}(S_\ell)\}} \\
&\geq \frac{\|\beta\|^2}{k \cdot \min\{\operatorname{vol}(S_j), \operatorname{vol}(S_\ell)\}} \cdot \left(\frac{2\pi \cdot |j - \ell|}{\lceil 2\pi \cdot k \rceil} \cdot \frac{2}{\pi} \right)^2 \\
&\geq \frac{\|\beta\|^2}{3k^3 \cdot \min\{\operatorname{vol}(S_j), \operatorname{vol}(S_\ell)\}},
\end{aligned}$$

where the second inequality holds by the fact that $\sin x \geq (2/\pi) \cdot x$ holds for any $x \in [0, \pi/2]$. This finishes the proof of the lemma. \square

The following lemma will be used to prove Theorem 4.4. We remark that the following proof closely follows the similar one from [23], however some constants need to be adjusted for our propose. We include the proof here for completeness.

Lemma B.1. *Let A_0, \dots, A_{k-1} be a partition of V . Assume that, for every permutation $\sigma : \{0, \dots, k-1\} \rightarrow \{0, \dots, k-1\}$, there exists some j' such that $\operatorname{vol}(A_{j'} \triangle S_{\sigma(j')}) \geq \varepsilon \operatorname{vol}(S_{\sigma(j')})$ for some $48 \cdot k^3 \cdot (1 + \text{APT}) / (\gamma_k(G) - 1) \leq \varepsilon \leq 1/2$, then $\text{COST}(A_0, \dots, A_{k-1}) \geq 2\text{APT} / (\gamma_k(G) - 1)$.*

Proof. We first consider the case where there exists a permutation $\sigma : \{0, \dots, k-1\} \rightarrow \{0, \dots, k-1\}$ such that, for any $0 \leq j \leq k-1$,

$$\operatorname{vol}(A_j \cap S_{\sigma(j)}) > \frac{1}{2} \operatorname{vol}(S_{\sigma(j)}). \tag{10}$$

This assumption essentially says that A_0, \dots, A_{k-1} is a non-trivial approximation of the optimal clustering S_0, \dots, S_{k-1} according to some permutation σ . Later we will show the statement of the lemma trivially holds if no permutations satisfy (10).

Based on this assumption, there is $0 \leq j' \leq k-1$ such that $\text{vol}(A_{j'} \triangle S_{\sigma(j')}) \geq 2\varepsilon \text{vol}(S_{\sigma(j')})$ for some $48 \cdot k^3 \cdot \text{APT} / (\gamma_k(G) - 1) \leq \varepsilon \leq 1/2$. Since

$$\begin{aligned} \text{vol}(A_{j'} \triangle S_{\sigma(j')}) &= \text{vol}(A_{j'} \setminus S_{\sigma(j')}) + \text{vol}(S_{\sigma(j')} \setminus A_{j'}) \\ &= \sum_{j \neq j'} \text{vol}(A_{j'} \cap S_{\sigma(j)}) + \sum_{j \neq j'} \text{vol}(S_{\sigma(j')} \cap A_j), \end{aligned}$$

one of the following two cases must hold:

1. A large portion of $A_{j'}$ belongs to clusters different from $S_{\sigma(j')}$, i.e., there exist $\varepsilon_0, \dots, \varepsilon_{k-1} \geq 0$ such that $\varepsilon_{j'} = 0$, $\sum_{j=0}^{k-1} \varepsilon_j \geq \varepsilon$, and $\text{vol}(A_{j'} \cap S_{\sigma(j)}) \geq \varepsilon_j \text{vol}(S_{\sigma(j')})$ for any $0 \leq j \leq k-1$.
2. $A_{j'}$ is missing a large portion of $S_{\sigma(j')}$, which must have been assigned to other clusters. Therefore, we can define $\varepsilon_0, \dots, \varepsilon_{k-1} \geq 0$ such that $\varepsilon_{j'} = 0$, $\sum_{j=0}^{k-1} \varepsilon_j \geq \varepsilon$, and $\text{vol}(A_j \cap S_{\sigma(j')}) \geq \varepsilon_j \text{vol}(S_{\sigma(j')})$ for any $0 \leq j \leq k-1$.

In both cases, we can define sets B_0, \dots, B_{k-1} and D_0, \dots, D_{k-1} such that B_j and D_j belong to the same cluster of the returned clustering but to two different optimal clusters S_{j_1} and S_{j_2} . More precisely, in the first case, for any $0 \leq j \leq k-1$, we define $B_j = A_{j'} \cap S_{\sigma(j)}$. We define D_0, \dots, D_{k-1} as an arbitrarily partition of $A_{j'} \cap S_{\sigma(j')}$ with the constraint that $\text{vol}(D_j) \geq \varepsilon_j \text{vol}(S_{\sigma(j')})$. This is possible since by (10)

$$\text{vol}(A_{j'} \cap S_{\sigma(j')}) \geq \frac{1}{2} \text{vol}(S_{\sigma(j')}) \geq \varepsilon \text{vol}(S_{\sigma(j')}).$$

In the second case, instead, for any $0 \leq j \leq k-1$, we define $B_j = A_j \cap S_{\sigma(j')}$ and $D_j = A_j \cap S_{\sigma(j)}$. Note that it also holds by (10) that $\text{vol}(D_j) \geq \varepsilon_j \text{vol}(S_{\sigma(j)})$. We can then combine the two cases together (albeit using different definitions for the sets) and assume that there exist $\varepsilon_0, \dots, \varepsilon_{k-1} \geq 0$ such that $\varepsilon_{j'} = 0$, $\sum_{j=0}^{k-1} \varepsilon_j \geq \varepsilon$, and such that we can find collections of pairwise disjoint sets $\{B_0, \dots, B_{k-1}\}$ and $\{D_0, \dots, D_{k-1}\}$ with the following properties: for any j there exist indices \bar{j} and $j_1 \neq j_2$ such that

1. $B_j, D_j \subseteq A_{\bar{j}}$
2. $D_j \subseteq S_{j_1}, B_j \subseteq S_{j_2}$
3. $\text{vol}(B_j) \geq \varepsilon_j \min\{\text{vol}(S_{j_1}), \text{vol}(S_{j_2})\}$
4. $\text{vol}(D_j) \geq \varepsilon_j \min\{\text{vol}(S_{j_1}), \text{vol}(S_{j_2})\}$

For any j , we define c_j as the centre of the corresponding cluster $A_{\bar{j}}$ to which both B_j and D_j are subset of. We can also assume without loss of generality that $\|c_j - p^{(j_1)}\| \geq \|c_j - p^{(j_2)}\|$ which implies

$$\|p^{(j_1)} - c_j\| \geq \frac{1}{2} \cdot \|p^{(j_1)} - p^{(j_2)}\|.$$

As a consequence, points in B_j are far away from c_j . Notice that if instead $\|c_j - p^{(j_1)}\| < \|c_j - p^{(j_2)}\|$, we would just need to reverse the role of B_j and D_j without changing the proof. We now bound $\text{COST}(A_0, \dots, A_{k-1})$ by looking only at the contribution of the points in the B_j 's. Therefore, we have that

$$\text{COST}(A_0, \dots, A_{k-1}) = \sum_{j=0}^{k-1} \sum_{u \in A_j} d_u \|F(u) - c_j\|^2 \geq \sum_{j=0}^{k-1} \sum_{u \in B_j} d_u \|F(u) - c_j\|^2.$$

By applying the inequality $a^2 + b^2 \geq (a - b)^2/2$, we have that

$$\begin{aligned}
\text{COST}(A_0, \dots, A_{k-1}) &\geq \sum_{j=0}^{k-1} \sum_{u \in B_j} d_u \left(\frac{\|p^{(j_1)} - c_j\|^2}{2} - \|F(u) - p^{(j_1)}\|^2 \right) \\
&\geq \sum_{j=0}^{k-1} \sum_{u \in B_j} d_u \frac{\|p^{(j_1)} - c_j\|^2}{2} - \sum_{j=0}^{k-1} \sum_{u \in B_j} d_u \|F(u) - p^{(j_1)}\|^2 \\
&\geq \sum_{j=0}^{k-1} \sum_{u \in B_j} d_u \frac{\|p^{(j_1)} - c_j\|^2}{2} - \frac{1}{\gamma_k(G) - 1} \\
&\geq \sum_{j=0}^{k-1} \sum_{u \in B_j} d_u \frac{\|p^{(j_1)} - p^{(j_2)}\|^2}{8} - \frac{1}{\gamma_k(G) - 1} \\
&\geq \sum_{j=0}^{k-1} \frac{\|\beta\|^2 \cdot \text{vol}(B_j)}{24k^3 \cdot \min\{\text{vol}(S_{j_1}), \text{vol}(S_{j_2})\}} - \frac{1}{\gamma_k(G) - 1} \\
&\geq \sum_{j=0}^{k-1} \frac{\|\beta\|^2 \cdot \varepsilon_j \min\{\text{vol}(S_{j_1}), \text{vol}(S_{j_2})\}}{24k^3 \cdot \min\{\text{vol}(S_{j_1}), \text{vol}(S_{j_2})\}} - \frac{1}{\gamma_k(G) - 1} \\
&\geq \sum_{j=0}^{k-1} \frac{\varepsilon_j \cdot \|\beta\|^2}{24k^3} - \frac{1}{\gamma_k(G) - 1} \\
&\geq \frac{\varepsilon}{24k^3} - \frac{1}{\gamma_k(G) - 1} \\
&\geq \frac{1}{24k^3} \cdot \frac{48k^3 \cdot (1 + \text{APT})}{\gamma_k(G) - 1} - \frac{1}{\gamma_k(G) - 1} \\
&\geq \frac{2\text{APT}}{\gamma_k(G) - 1}.
\end{aligned}$$

It remains to show that removing assumption (10) implies the Lemma as well. Notice that if (10) is not satisfied, for all permutations σ there exists $0 \leq \ell^* \leq k - 1$ such that $\text{vol}(A_{\ell^*} \cap S_{\sigma(\ell^*)}) \leq \frac{1}{2} \text{vol}(S_{\sigma(\ell^*)})$. We can also assume the following stronger condition:

$$\text{vol}(A_{\ell^*} \cap S_j) \leq \frac{1}{2} \text{vol}(S_j) \quad \text{for any } 0 \leq j \leq k - 1. \quad (11)$$

Indeed, if there would exist a unique $j \neq \sigma(\ell^*)$ such that $\text{vol}(A_{\ell^*} \cap S_j) > \frac{1}{2} \text{vol}(S_j)$, then it would just mean that σ is the “wrong” permutation and we should consider only permutations $\sigma' \neq \sigma$ such that $\sigma'(\ell^*) = j$. If instead there would exist $j_1 \neq j_2$ such that $\text{vol}(A_{\ell^*} \cap S_{j_1}) > \frac{1}{2} \text{vol}(S_{j_1})$ and $\text{vol}(A_{\ell^*} \cap S_{j_2}) > \frac{1}{2} \text{vol}(S_{j_2})$, then it is easy to see that the Lemma would hold, since in this case A_{ℓ^*} would contain large portions of two different optimal clusters, and, as clear from the previous part of the proof, this would imply a high k -means cost.

Therefore, we just need to show that the statement of the Lemma holds when (11) is satisfied. For this purpose we define sets C_0, \dots, C_{k-1} which are subsets of vertices in S_0, \dots, S_{k-1} that are close in the spectral embedding to $p^{(0)}, \dots, p^{(k-1)}$. Formally, for any $0 \leq j \leq k - 1$,

$$C_j = \left\{ u \in S_j : \|F(u) - p^{(j)}\|^2 \leq \frac{100}{\text{vol}(S_j)} \cdot (\gamma_k(G) - 1) \right\}.$$

Notice that by Lemma 4.1 $\text{vol}(C_j) \geq \frac{99}{100} \text{vol}(S_j)$. By assumption (11), roughly half of the volume of all the C_j ’s must be contained in at most $k - 1$ sets (all the A_j ’s different from A_{ℓ^*}). We prove this implies that the k -means cost is high, from which the Lemma follows.

Let c_0, \dots, c_{k-1} be the centres of A_0, \dots, A_{k-1} . We are trying to assign a large portion of each of the k optimal clusters to only $k - 1$ centres (namely all the centres different from c_{ℓ^*}). Moreover,

any centre $c_j \neq c_{\ell^*}$ can either be close to $p^{(\ell^*)}$ or to another optimal centre $p^{(j')}$, but not to both. As a result, there will be at least one C_j whose points are assigned to a centre which is at least $\Omega(1/\text{vol}(S_j))$ far from $p^{(j)}$ (in squared Euclidean distance). Therefore, by the definition of C_j and the fact that $\text{vol}(C_j) \geq \frac{99}{100} \text{vol}(S_j)$, the k -means cost is at least $\Omega\left(\frac{1}{\text{vol}(S_j)} \cdot \text{vol}(C_j)\right) = \Omega(1)$. This concludes the proof. \square

Proof of Theorem 4.4. Assume for contradiction that, for any permutation $\sigma : \{0, \dots, k-1\} \rightarrow \{0, \dots, k-1\}$, there is an index $j \in \{0, \dots, k-1\}$ such that $\text{vol}(A_j \triangle S_{\sigma(j)}) \geq \varepsilon \text{vol}(S_{\sigma(j)})$. Then, by Lemma B.1 we have that $\text{COST}(A_0, \dots, A_{k-1}) \geq 2\text{APT} / (\gamma_k(G) - 1)$, which contradicts the fact that $\text{COST}(A_0, \dots, A_{k-1}) \leq \text{APT} / (\gamma_k(G) - 1)$. \square

Now we prove Theorem 4.5. The following two technical lemmas will be used in our proof.

Lemma B.2 (Bernstein's Inequality, [8]). *Let X_1, \dots, X_n be independent random variables such that $|X_i| \leq M$ for any $i \in \{1, \dots, n\}$. Let $X = \sum_{i=1}^n X_i$ and let $R = \sum_{i=1}^n \mathbb{E}[X_i^2]$. Then, it holds that*

$$\mathbb{P}[|X - \mathbb{E}[X]| \geq t] \leq 2 \cdot \exp\left(-\frac{t^2}{2(R + Mt/3)}\right).$$

Lemma B.3 (Matrix Chernoff Bound, [28]). *Consider a finite sequence $\{X_i\}$ of independent, random, PSD matrices of dimension d that satisfy $\|X_i\| \leq R$. Let $\mu_{\min} \triangleq \lambda_{\min}(\mathbb{E}[\sum_i X_i])$ and $\mu_{\max} \triangleq \lambda_{\max}(\mathbb{E}[\sum_i X_i])$. Then it holds that*

$$\begin{aligned} \mathbb{P}\left[\lambda_{\min}\left(\sum_i X_i\right) \leq (1-\delta)\mu_{\min}\right] &\leq d \cdot \left(\frac{e^{-\delta}}{(1-\delta)^{1-\delta}}\right)^{\mu_{\min}/R} \text{ for } \delta \in [0, 1], \text{ and} \\ \mathbb{P}\left[\lambda_{\max}\left(\sum_i X_i\right) \geq (1+\delta)\mu_{\max}\right] &\leq d \cdot \left(\frac{e^{\delta}}{(1+\delta)^{1+\delta}}\right)^{\mu_{\max}/R} \text{ for } \delta \geq 0. \end{aligned}$$

Proof of Theorem 4.5. We first analyse the size of F . Since

$$\sum_{u \in V} \sum_{e=(u,v)} w(u,v) \cdot \frac{\alpha \log n}{d_u^{\text{out}} \cdot \lambda_2} = O\left(\frac{n \log n}{\lambda_2}\right),$$

and

$$\sum_{v \in V} \sum_{e=(u,v)} w(u,v) \cdot \frac{\alpha \log n}{d_v^{\text{in}} \cdot \lambda_2} = O\left(\frac{n \log n}{\lambda_2}\right),$$

it holds by Markov inequality that the number of edges $e = (u, v)$ with $w(u, v) \cdot \frac{\alpha \log n}{d_u^{\text{out}} \cdot \lambda_2} \geq 1$ and $w(u, v) \cdot \frac{\alpha \log n}{d_v^{\text{in}} \cdot \lambda_2} \geq 1$ is $O\left(\frac{n \log n}{\lambda_2}\right)$. Without loss of generality, we assume that these edges are in F , and in the remaining part of the proof we assume it holds for any edge $e = (u, v)$ that

$$w(u, v) \cdot \frac{\alpha \cdot \log n}{d_u^{\text{out}} \cdot \lambda_2} < 1, \quad w(u, v) \cdot \frac{\alpha \cdot \log n}{d_v^{\text{in}} \cdot \lambda_2} < 1.$$

Moreover, the expected number of edges in H equals to

$$\begin{aligned} \sum_{e=(u,v)} p_e &\leq \sum_{e=(u,v)} p_u(u, v) + p_v(u, v) = \frac{\alpha \cdot \log n}{\lambda_2} \sum_{e=(u,v)} \left(\frac{w(u, v)}{d_u^{\text{out}}} + \frac{w(u, v)}{d_v^{\text{in}}}\right) \\ &= O\left(\frac{n \log n}{\lambda_2}\right), \end{aligned}$$

and thus by Markov's inequality we have that with constant probability the number of sampled edges $|F| = O((1/\lambda_2) \cdot n \log n)$.

Proof of $\theta_k(H) = \Omega(\theta_k(G))$. Next we show that the sparsified graph constructed by the algorithm preserves $\theta_k(G)$ up to a constant factor. Without loss of generality, let S_0, \dots, S_{k-1} be the optimal k clusters such that

$$\Phi_G(S_0, \dots, S_{k-1}) = \theta_k(G).$$

For any edge $e = (u, v)$ satisfying $u \in S_j$ and $v \in S_{j-1}$ for some $1 \leq j \leq k-1$, we define a random variable Y_e by

$$Y_e = \begin{cases} w(u, v)/p_e & \text{with probability } p_e, \\ 0 & \text{otherwise.} \end{cases}$$

We also define random variables Z_1, \dots, Z_{k-1} , where Z_j ($1 \leq j \leq k-1$) is defined by

$$Z_j = \sum_{\substack{e=\{u,v\} \in E[G] \\ u \in S_j, v \in S_{j-1}}} Y_e.$$

By definition, we have that

$$\mathbb{E}[Z_j] = \sum_{\substack{e=\{u,v\} \in E[G] \\ u \in S_j, v \in S_{j-1}}} \mathbb{E}[Y_e] = \sum_{\substack{e=\{u,v\} \in E[G] \\ u \in S_j, v \in S_{j-1}}} w(u, v) = w(S_j, S_{j-1}).$$

Moreover, we look at the second moment and have that

$$\begin{aligned} \sum_{\substack{e=\{u,v\} \in E[G] \\ u \in S_j, v \in S_{j-1}}} \mathbb{E}[Y_e^2] &= \sum_{\substack{e=\{u,v\} \in E[G] \\ u \in S_j, v \in S_{j-1}}} p_e \cdot \left(\frac{w(u, v)}{p_e} \right)^2 \\ &= \sum_{\substack{e=\{u,v\} \in E[G] \\ u \in S_j, v \in S_{j-1}}} \frac{(w(u, v))^2}{p_e} \\ &\leq \sum_{\substack{e=\{u,v\} \in E[G] \\ u \in S_j, v \in S_{j-1}}} \frac{(w(u, v))^2}{w(u, v)} \cdot \frac{\lambda_2 \cdot d_u^{\text{out}}}{\alpha \log n} \\ &= \frac{\lambda_2}{\alpha \log n} \cdot \sum_{\substack{e=\{u,v\} \in E[G] \\ u \in S_j, v \in S_{j-1}}} w(u, v) \cdot d_u^{\text{out}} \\ &\leq \frac{\lambda_2}{\alpha \log n} \cdot \Delta_j^{\text{out}} \cdot w(S_j, S_{j-1}), \end{aligned}$$

where Δ_j^{out} is the maximum of the out degree of vertices in S_j and the first inequality follows by the fact that

$$p_e = p_u(u, v) + p_v(u, v) - p_u(u, v)p_v(u, v) \geq p_u(u, v) = w(u, v) \cdot \frac{\alpha \log n}{\lambda_2 \cdot d_u^{\text{out}}}.$$

In addition, it holds for any $e = (u, v)$, $u \in S_j$, $v \in S_{j-1}$ that

$$\left| \frac{w(u, v)}{p_e} \right| \leq \left| \frac{w(u, v)}{p_u(u, v)} \right| \leq \frac{\lambda_2 \cdot \Delta_j^{\text{out}}}{\alpha \cdot \log n}.$$

We apply Bernstein's Inequality (Lemma B.2), and obtain for any $1 \leq j \leq k-1$ that

$$\begin{aligned} &\mathbb{P}[|Z_j - w(S_j, S_{j-1})| \geq (1/2) \cdot w(S_j, S_{j-1})] \\ &= \mathbb{P}[|Z_j - \mathbb{E}[Z_j]| \geq (1/2) \cdot \mathbb{E}[Z_j]] \\ &\leq 2 \cdot \exp \left(- \frac{\mathbb{E}[Z_j]^2/4}{2 \left(\frac{\lambda_2}{\alpha \log n} \cdot \Delta_j^{\text{out}} \cdot w(S_j, S_{j-1}) + \frac{\lambda_2 \cdot \Delta_j^{\text{out}}}{\alpha \cdot \log n} \cdot \frac{1}{6} \cdot w(S_j, S_{j-1}) \right)} \right) \\ &\leq 2 \cdot \exp \left(- \frac{\alpha \cdot \log n \cdot \mathbb{E}[Z_j]}{10 \cdot \lambda_2 \cdot \Delta_j^{\text{out}}} \right). \end{aligned}$$

Hence, with high probability cut values $w(S_j, S_{j-1})$ for all $1 \leq j \leq k-1$ are approximated up to a constant factor. Using the same technique, we can show that with high probability the volumes of all

the sets S_0, \dots, S_{k-1} are approximately preserved in H as well. Combining this with the definition of Φ , we have that $\Phi_G(S_0, \dots, S_{k-1})$ and $\Phi_H(S_0, \dots, S_{k-1})$ are approximately the same up to a constant factor. Since S_0, \dots, S_{k-1} are the sets that maximising the value of $\theta_k(G)$, we have that $\theta_k(H) = \Omega(\theta_k(G))$.

Proof of $\lambda_2(\mathcal{L}_H) = \Omega(\lambda_2(\mathcal{L}_G))$. Finally, we prove that the top $n - 1$ eigenspace is approximately preserved in H . Let $\bar{\mathcal{L}}_G$ be the projection of \mathcal{L}_G on its top $n - 1$ eigenspaces. We can write $\bar{\mathcal{L}}_G$ as

$$\bar{\mathcal{L}}_G = \sum_{i=2}^n \lambda_i f_i f_i^*.$$

With a slight abuse of notation we call $\bar{\mathcal{L}}_G^{-1/2}$ the square root of the pseudoinverse of $\bar{\mathcal{L}}_G$, i.e.,

$$\bar{\mathcal{L}}_G^{-1/2} = \sum_{i=2}^n (\lambda_i)^{-1/2} f_i f_i^*.$$

We call $\bar{\mathcal{L}}$ the projection on $\text{span}\{f_2, \dots, f_n\}$, i.e.,

$$\bar{\mathcal{L}} = \sum_{i=2}^n f_i f_i^*.$$

We will prove that the top $n - 1$ eigenspaces of \mathcal{L}_G are preserved. To prove this, recall that the probability of any edge $e = (u, v)$ being sampled in H is

$$p_e = p_u(u, v) + p_v(u, v) - p_u(u, v) \cdot p_v(u, v),$$

and it holds that $\frac{1}{2}(p_u(u, v) + p_v(u, v)) \leq p_e \leq p_u(u, v) + p_v(u, v)$. Now for each edge $e = (u, v)$ of G we define a random matrix $X_e \in \mathbb{C}^{n \times n}$ by

$$X_e = \begin{cases} w_H(u, v) \cdot \bar{\mathcal{L}}_G^{-1/2} b_e b_e^* \bar{\mathcal{L}}_G^{-1/2} & \text{if } e = (u, v) \text{ is sampled by the algorithm,} \\ 0 & \text{otherwise,} \end{cases}$$

where the vector b_e is defined by $b_e = \left(\omega_{2\lceil 2\pi \cdot k \rceil} \chi_u - \omega_{2\lceil 2\pi \cdot k \rceil}^* \chi_v \right)$ and for any vertex u the normalised indicator vector χ_u is defined by $\chi_u(u) = 1/\sqrt{d_u}$, and $\chi_u(v) = 0$ for any $v \neq u$. Notice that

$$\sum_{e \in E[G]} X_e = \sum_{\text{sampled edges } e=(u,v)} w_H(u, v) \cdot \bar{\mathcal{L}}_G^{-1/2} b_e b_e^* \bar{\mathcal{L}}_G^{-1/2} = \bar{\mathcal{L}}_G^{-1/2} \mathcal{L}'_H \bar{\mathcal{L}}_G^{-1/2},$$

where it follows by definition that

$$\mathcal{L}'_H = \sum_{\text{sampled edges } e=(u,v)} w_H(u, v) \cdot b_e b_e^*$$

is essentially the Laplacian matrix of H but is normalised with respect to the degrees of the vertices in the original graph G , i.e., $\mathcal{L}'_H = D_G^{-1} D_H - D_G^{-1/2} A_H D_G^{-1/2}$. We will prove that, with high probability, the top $n - 1$ eigenspaces of \mathcal{L}'_H and \mathcal{L}_G are approximately the same. Later we will show the same holds for \mathcal{L}_H and \mathcal{L}'_H , which implies that $\lambda_2(\mathcal{L}'_H) = \Omega(\lambda_2(\mathcal{L}_G))$.

We will use the matrix Chernoff bound for our proof. We start looking at the first moment of the expression above:

$$\begin{aligned} \mathbb{E} \left[\sum_{e \in E} X_e \right] &= \sum_{e=(u,v) \in E[G]} p_e \cdot w_H(u, v) \cdot \bar{\mathcal{L}}_G^{-1/2} b_e b_e^* \bar{\mathcal{L}}_G^{-1/2} \\ &= \sum_{e=(u,v) \in E[G]} p_e \cdot \frac{w(u, v)}{p_e} \cdot \bar{\mathcal{L}}_G^{-1/2} b_e b_e^* \bar{\mathcal{L}}_G^{-1/2} \\ &= \bar{\mathcal{L}}_G^{-1/2} \mathcal{L}_G \bar{\mathcal{L}}_G^{-1/2} = \bar{\mathcal{L}}. \end{aligned}$$

Moreover, for any sampled $e = (u, v) \in E$ we have that

$$\begin{aligned} \|X_e\| &\leq w_H(u, v) \cdot b_e^* \bar{\mathcal{L}}_G^{-1/2} \bar{\mathcal{L}}_G^{-1/2} b_e = \frac{w(u, v)}{p_e} \cdot b_e^* \bar{\mathcal{L}}_G^{-1} b_e \leq \frac{w(u, v)}{p_e} \cdot \frac{1}{\lambda_2} \cdot \|b_e\|^2 \\ &\leq \frac{2\lambda_2}{\alpha \cdot \log n \cdot \left(\frac{1}{d_u^{\text{out}}} + \frac{1}{d_v^{\text{in}}}\right)} \cdot \frac{1}{\lambda_2} \left(\frac{1}{d_u^{\text{out}}} + \frac{1}{d_v^{\text{in}}}\right) \leq \frac{2}{\alpha \log n}, \end{aligned}$$

where the second inequality follows by the min-max theorem of eigenvalues. Now we apply the matrix Chernoff bound (Lemma B.3) to analyse the eigenvalues of $\sum_{e \in E} X_e$, and build a connection between $\lambda_2(\mathcal{L}'_H)$ and $\lambda_2(\mathcal{L}_G)$. By setting the parameters of Lemma B.3 by $\mu_{\max} = \lambda_{\max} \left(\mathbb{E} \left[\sum_{e \in E[G]} X_e \right] \right) = \lambda_{\max}(\bar{\mathcal{L}}) = 1$, $R = 2/(\alpha \cdot \log n)$ and $\delta = 1/2$, we have that

$$\mathbb{P} \left[\lambda_{\max} \left(\sum_{e \in E[G]} X_e \right) \geq 3/2 \right] \leq n \cdot \left(\frac{e^{1/2}}{(1 + 1/2)^{3/2}} \right)^{\alpha \log n / 2} = O(1/n^c)$$

for some constant c . This gives us that

$$\mathbb{P} \left[\lambda_{\max} \left(\sum_{e \in E[G]} X_e \right) \leq 3/2 \right] = 1 - O(1/n^c). \quad (12)$$

On the other side, since our goal is to analyse $\lambda_2(\mathcal{L}'_H)$ with respect to $\lambda_2(\mathcal{L}_G)$, it suffices to work with the top $(n - 1)$ eigenspace of \mathcal{L}_G . Since $\mathbb{E} \left[\sum_{e \in E} X_e \right] = \bar{\mathcal{L}}$, we can assume without loss of generality that $\mu_{\min} = 1$. Hence, by setting $R = 2/(\alpha \cdot \log n)$ and $\delta = 1/2$, we have that

$$\mathbb{P} \left[\lambda_{\min} \left(\sum_{e \in E[G]} X_e \right) \leq 1/2 \right] = n \cdot \left(\frac{e^{-1/2}}{(1/2)^{1/2}} \right)^{\alpha \log n / 2} = O(1/n^c)$$

for some constant c . This gives us that

$$\mathbb{P} \left[\lambda_{\min} \left(\sum_{e \in E[G]} X_e \right) > 1/2 \right] = 1 - O(1/n^c). \quad (13)$$

Combining (12), (13), and the fact of $\sum_{e \in E[G]} X_e = \bar{\mathcal{L}}_G^{-1/2} \mathcal{L}'_H \bar{\mathcal{L}}_G^{-1/2}$, with probability $1 - O(1/n^c)$ it holds for any non-zero $x \in \mathbb{C}^n$ in the space spanned by f_2, \dots, f_n that

$$\frac{x^* \bar{\mathcal{L}}_G^{-1/2} \mathcal{L}'_H \bar{\mathcal{L}}_G^{-1/2} x}{x^* x} \in (1/2, 3/2). \quad (14)$$

By setting $y = \bar{\mathcal{L}}_G^{-1/2} x$, we can rewrite (14) as

$$\frac{y^* \mathcal{L}'_H y}{y^* \bar{\mathcal{L}}_G^{-1/2} \bar{\mathcal{L}}_G^{-1/2} y} = \frac{y^* \mathcal{L}'_H y}{y^* \bar{\mathcal{L}}_G y} = \frac{y^* \mathcal{L}'_H y}{y^* y} \frac{y^* y}{y^* \bar{\mathcal{L}}_G y} \in (1/2, 3/2).$$

Since $\dim(\text{span}\{f_2, \dots, f_n\}) = n - 1$, we have just proved there exist $n - 1$ orthogonal vectors whose Rayleigh quotient with respect to \mathcal{L}'_H is $\Omega(\lambda_2(\mathcal{L}_G))$. By the Courant-Fischer Theorem, we have

$$\lambda_2(\mathcal{L}'_H) \geq \frac{1}{2} \lambda_2(\mathcal{L}_G). \quad (15)$$

It remains to show that $\lambda_2(\mathcal{L}_H) = \Omega(\lambda_2(\mathcal{L}'_H))$, which implies that $\lambda_2(\mathcal{L}_H) = \Omega(\lambda_2(\mathcal{L}_G))$ by (15). By the definition of \mathcal{L}'_H , we have that for the Laplacian $\mathcal{L}_H = D_H^{-1/2} D_G^{1/2} \mathcal{L}'_H D_G^{1/2} D_H^{-1/2}$. Therefore, for any $x \in \mathbb{C}^n$ and $y = D_G^{1/2} D_H^{-1/2} x$, it holds that

$$\frac{x^* \mathcal{L}_H x}{x^* x} = \frac{y^* \mathcal{L}'_H y}{y^* y} \geq \frac{1}{2} \cdot \frac{y^* \mathcal{L}'_H y}{y^* y}, \quad (16)$$

where the last equality follows from the fact that the degrees in H and G differ just by a constant multiplicative factor, and therefore,

$$y^*y = \left(D_G^{1/2}D_H^{-1/2}x\right)^* \left(D_G^{1/2}D_H^{-1/2}x\right) = x^*D_GD_H^{-1}x \geq \frac{1}{2} \cdot x^*x.$$

Finally, we show that (16) implies that $\lambda_2(\mathcal{L}_H) \geq (1/2) \cdot \lambda_2(\mathcal{L}'_H)$. To see this, let $S_1 \subseteq \mathbb{C}^n$ be a (2)-dimensional subspace of \mathbb{C}^n such that

$$\lambda_2(\mathcal{L}_H) = \max_{x \in S_1} \frac{x^*\mathcal{L}_Hx}{x^*x}.$$

Let $S_2 = \left\{D_G^{1/2}D_H^{-1/2}x : x \in S_1\right\}$. Notice that since $D_G^{1/2}D_H^{-1/2}$ is full rank, S_2 has dimension 2. Therefore,

$$\lambda_2(\mathcal{L}'_H) = \min_{S: \dim(S)=2} \max_{y \in S} \frac{y^*\mathcal{L}'_Hy}{y^*y} \leq \max_{y \in S_2} \frac{y^*\mathcal{L}'_Hy}{y^*y} \leq 2 \max_{x \in S_1} \frac{x^*\mathcal{L}_Hx}{x^*x} = 2\lambda_2(\mathcal{L}_H), \quad (17)$$

where the last inequality follows by (16). Combining (15) with (17) gives us that $\lambda_2(\mathcal{L}_H) = \Omega(\lambda_2(G))$. This concludes the proof. \square

C Omitted details from Section 5

C.1 UN Comtrade Data Preparation

The API provided by the UN gives a lot of flexibility on the type of selected data. It is possible to specify the *product type* to either trade in goods (e.g., oil, wood, and appliances) or services (e.g., financial services, and construction services). Moreover, the *classification code* can be selected, which we set to the Harmonised System (HS). The HS categorises goods according to a 6-digit classification code (e.g., 060240, where the first two digits “06” represents “plants”, the second two digits “02” represents “alive”, and the last two digits “40” code for “roses”). The *reporting* countries and *partner* countries can also be specified, where the reporting country reports about its own reported trade flow with partner countries. The settings we used to download the data for our experiments were Goods on an annual frequency, the HS code as reported, over the period from 2002 to 2017, with all reporting and all partner countries, all trade flows and all HS commodity codes. The total size of the data in zipped files is 99.8GB, where each csv file (for every year) contains around 20,000,000 lines.

For every pair of countries j and ℓ , where j is the reporting country and ℓ is the partner country, the database contains the amount that country j imports from country ℓ for a specific commodity, and also the amount j exports to ℓ . There are several cases where countries j and ℓ report different trading amounts with each other. Usually, the larger value is considered more accurate and is used instead of the average [12]. To construct the digraph of the world trade network and its corresponding adjacency matrix, we fill in each entry of the adjacency matrix M^c for commodity c as follows: for each pair of countries j and ℓ , we compute $d_{j\ell}^c = e_{j\ell}^c - e_{\ell j}^c$, where $e_{j\ell}^c$ is the amount country j exports to country ℓ for commodity c . If $d_{j\ell}^c > 0$, we set $M_{j\ell}^c = d_{j\ell}^c$ and $M_{\ell j}^c = 0$. If $d_{j\ell}^c < 0$ (and thus $d_{\ell j}^c > 0$), we set $M_{\ell j}^c = d_{\ell j}^c$ and $M_{j\ell}^c = 0$.

For our experiments we investigate the trade in “Mineral Fuels, mineral oils, and products of their distillation” (HS code 27), and the trade in “Wood and articles of wood” (HS code 44).

C.2 DD-SYM Plots International Oil Trade

We plot the cluster visualisations for the DD-SYM algorithm in Figure 6 on the international oil trade network, over the period 2006-2009. The clusters between 2006 and 2007 are almost identical, and then there is a shift in the clustering structure between 2007 and 2008. This change occurs one year before the change in the SimpleHerm method, and this change is also one year earlier than the changes found in the complex network analysis literature [1, 33]. This indicates that the SimpleHerm clustering result is more in line with other literature.

C.3 International Wood Trade

For comparison we visualise the clustering result of the DD-SYM method over the period of 2006 – 2009, see Figure 7. In addition, Figure 8 compares the symmetric difference of the clusters returned

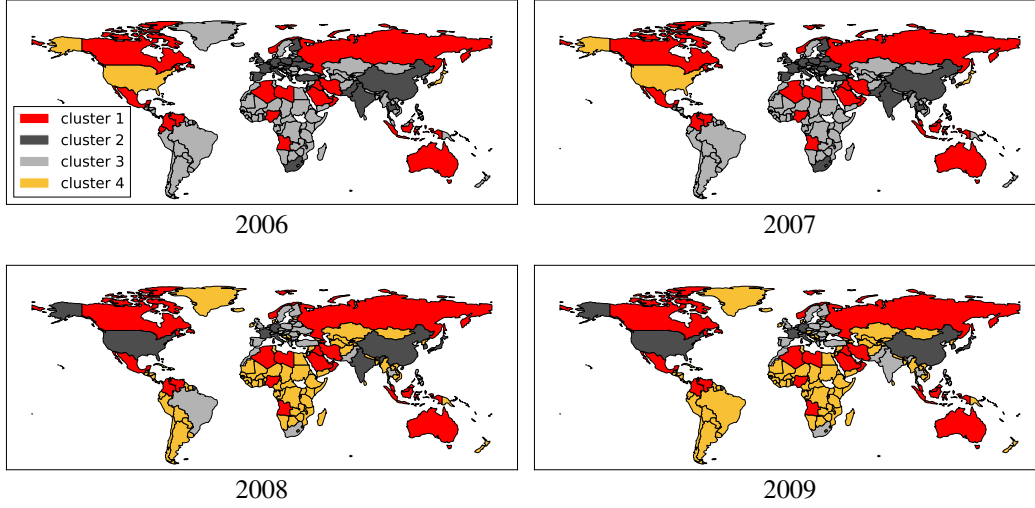


Figure 6: Change in clustering of the IOTN over period 2006–2009 with $k = 4$ using DD-SYM method. Red countries form the start of the trade chain, and yellow countries the end of the trade chain. Countries coloured white have no data.

by different algorithms over the consecutive years. Again, we notice that our algorithm finds a peak around the economic crisis of 2008, and another peak is found between 2005 and 2006. We could not find any literature reasoning about the peak between 2005 and 2006, but it would be interesting to analyse this further. The symmetric difference returned by the DD-SYM method is more noisy.

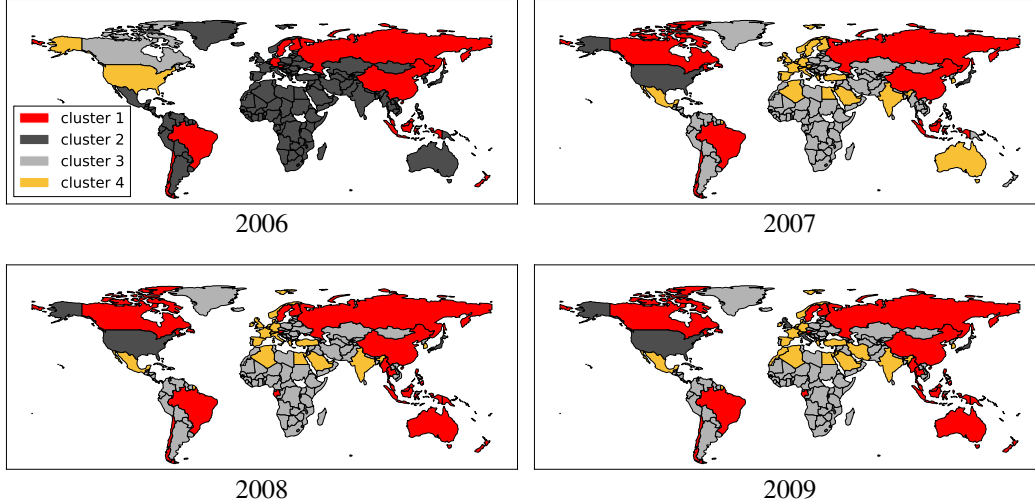


Figure 7: Change in clustering of the IWTN over period 2006–2009 with $k = 4$ using DD-SYM method. Red countries form the start of the trade chain, and yellow countries the end of the trade chain. Countries coloured white have no data.

C.4 Results on Data Science for COVID-19 Dataset

The *Data Science for COVID-19 Dataset* (DS4C) [19] contains information about 3519 South Korean COVID-19 cases, and we use directed edges to represent how the virus is transmitted among the individuals. We notice that there are only 831 edges in the graph and there are many connected components of size 2. To take this into account, we run our algorithm on the largest connected component of the infection graph, which consists of 67 vertices and 66 edges. Applying the complex-

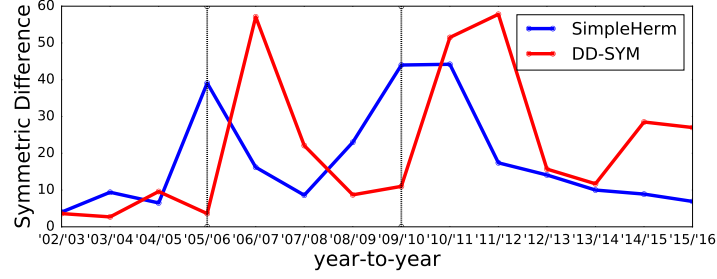


Figure 8: Comparison of the symmetric difference of the returned clusters between two consecutive years on the IWTN.

valued Hermitian matrix and the eigenvector associated with the smallest eigenvalue, the spectral embedding is visualised in Figure 9.

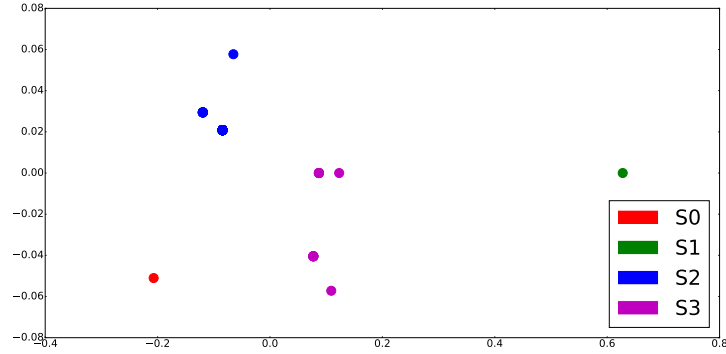


Figure 9: Clustering output on the largest connected component of the DS4C dataset, where $k = 4$. Clusters are labelled according to their position in the ordering that maximises the flow ratio.

We notice several interesting facts. First of all, we do not see all the individual nodes of the graph in this embedding. This is because many embedded points are overlapped, which happens if they have the same in and outgoing edges. Moreover, from cluster S_0 to S_1 there is 1 edge, from S_1 to S_2 there are 51 edges and from S_2 to S_3 there are 5 edges. That means there are $1 + 51 + 5 = 57$ edges that lie along the path, out of 66 edges in total. This concludes that our algorithm has successfully clustered the vertices such that there is a large flow ratio along the clusters.

Secondly, due to the limited size of the dataset, it is difficult for us to draw a more significant conclusion from the experiment. However, we do notice that the cluster S_1 actually consists of one individual: a super spreader. This individual infected 51 people in cluster S_2 . We believe that, with the development of many tracing Apps across the world and more data available in the near future, our algorithm could become a useful tool for disease tracking and policy making.